

Continued advancement of laser damage resistant optically functional microstructures.

Douglas S. Hobbs*, Bruce D. MacLeod, Ernest Sabatino III
TelAztec LLC, 15 A Street, Burlington, MA, USA 01803-3404

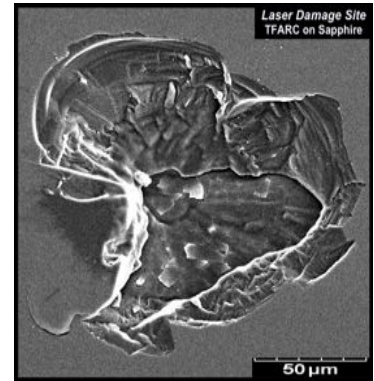
ABSTRACT

Micro- and nano-structured optically functional surface textures continue to exhibit higher performance and longer term survivability than thin-film coatings for an increasing number of materials used within high energy laser (HEL) systems. Anti-reflection (AR) microstructures (ARMs) produce a graded refractive index yielding high transmission over wide spectral ranges along with a chemical, mechanical and laser damage resistance inherited from the bulk optic material. In this study, ARMs were fabricated in the relevant HEL materials sapphire, neodymium-doped YAG, fused silica, BK7 glass, and the magnesium aluminate known as SPINEL. Standardized pulsed laser induced damage threshold (LiDT) measurements were made using commercial testing services to directly compare the damage resistance of ARMs-treated optics to uncoated and thin-film-AR-coated (TFARC) optics at wavelengths of 532nm, 694nm, 800nm, 1064nm, and 1538nm. As found with prior work, the LiDT of ARMs etched in fused silica was typically in the range of 35 J/cm² at a wavelength of 1064nm and a pulse width of 10ns, a level that is comparable to uncoated samples and 3.5 times greater than the level specified by six prominent TFARC providers. The Army Research Laboratory measured the pulsed LiDT at 532nm (10ns) of ARMs in fused silica to be up to 5 times the level of the ion beam sputtered TFARC previously employed in their HEL system, and 2 times higher than a low performance single layer MgF₂ TFARC. This result was repeated and expanded using a commercial LiDT testing service for ARMs in two types of fused silica and for Schott N-BK7 glass. An average damage threshold of 26.5 J/cm² was recorded for the ARMs-treated glass materials, a level 4 times higher than the commercial IBS TFARCs tested.

Keywords: HEL, High Energy Lasers, Antireflection, AR, Motheye, Nano-Texture, LIDT, Thin-Film AR Coatings

1.0 INTRODUCTION

An ongoing problem affecting the survivability of optical elements within high energy laser (HEL) systems is the limited performance and low damage resistance of thin-film material coatings used to impart optical functions such as anti-reflection (AR) and high- or partial reflection (HR or PR). A primary example of this problem as illustrated in the scanning electron micrograph (SEM) image on the right, is the consistently low laser induced damage threshold (LiDT) measured for thin-film AR coatings (TFARC). Specifically for fused silica optics, thin-film coating pulsed laser damage thresholds less than half the uncoated, as polished, material are commonly reported.^[1-3] In kilowatt and megawatt class HEL systems such as diode pumped alkali (DPAL) and chemical oxygen iodine (COIL) lasers, thin-film coating damage is often accelerated due to exposure to harsh chemical environments.^[4,5] Increased thin-film material absorption upon exposure to intense UV light and high electron beam flux limits the power scaling in free-electron laser (FEL) platforms.^[6] Loss of adhesion, limited bandwidth, and water vapor absorption^[7] in coatings severely limit the tuning ability of HEL systems designed for infrared countermeasures, optical communications, and medical applications.^[8,9] Differential absorption between coatings and solid state gain media can aggravate thermal lensing (or “self-focusing”) problems forcing a design with reduced output power as a tradeoff for mission survivability.



An innovative solution to these problems is to replace thin film coatings with surface relief microstructures fabricated directly into the facets of durable optical materials such as fused quartz, and yttrium aluminum garnet (YAG). AR, HR, PR, and even polarizing functions can be produced with microstructure arrays – textures that are non-scattering, and non-diffractive with feature dimensions much smaller than the wavelengths of light in a HEL system - where the optical performance and inherent durability of ten far exceeds that of thin-film coatings.^[10-13] In particular, AR microstructures (ARMs) that suppress reflections by a graded index effect rather than the constructive and destructive interference effect used by coatings, present no abrupt interfaces or dissimilar materials to a propagating light beam, and can therefore

* dshobbs@telaztec.com; phone 1 781 229-9905; www.telaztec.com

operate over a wide spectral range and wide field of regard retaining the same physical properties of the material in which they are built. Prior LiDT data for fused silica, glass, diamond, gallium arsenide (GaAs), and sapphire indicate that the damage resistance of ARMs-treated windows can be equivalent to the untreated material, potentially increasing the pulsed laser power handling capacity of HEL systems up to 4 times the level provided by thin-film coatings.^[14-21]

2.0 BACKGROUND: AR MICROSTRUCTURE TECHNOLOGY

Commonly known as *Motheys* in the literature^[22], ARMs textures have been demonstrated in a wide range of materials. Figure 1 shows overhead and elevation SEM images of 3 types of ARMs textures that have been fabricated in YAG, fused silica, sapphire, arsenic selenide (As_2Se_3), diamond, and BK7 glass windows. Periodic arrays of holes or posts are referred to as SWS-type (“sub-wavelength structures”) ARMs and are represented by the YAG^[19] and fused silica^[16-17] images on the left. Extremely high peak performance has been demonstrated for SWS AR textures in fused silica, measuring just 0.05% (-35dB) loss at 1.31 μm and 1.55 μm wavelengths^[16]. SWS textures in quartz^[19] have been demonstrated with <0.5% average reflection loss over the wavelength range of from 0.75 to 2.5 μm with less than 0.1% reflection loss at 1.064 μm . Traditional Motheys textures consisting of a periodic array of cones, are represented sequentially in the central three images for sapphire^[18-19], As_2Se_3 ^[20], and diamond^[18]. Motheys textures in sapphire have been measured with a transmission greater than 99.5% over the entire near IR (NIR) wavelength range of 1-2 μm . Motheys textures in ZnSe, CdZnTe, and As_2S_3 have exhibited even higher performance over the mid-IR wavelength band from 2-6 μm ^[20]. Randomly distributed cone-like features in Schott N-BK7 glass are shown in the right most images. “Random” ARMs textures in fused silica have exceptional bandwidths and peak performance values averaging less than 0.3% loss over the ultraviolet (UV) through NIR spectral range from 0.2 to 0.9 μm , or the visible-NIR range of 0.4-2.0 μm , with 0.05% loss at selected wavelengths within the 0.6-1.55 μm range^[16].

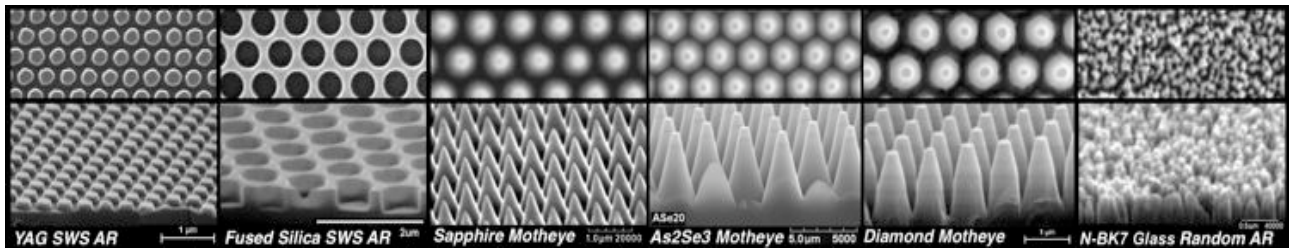
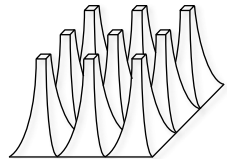


Figure 1: Overhead (top) and Elevation (bottom) SEM views of ARMs etched in the surface of 6 important optical materials.

2.1 ARMs TEXTURE DESIGN MODELING

Computer simulations based on rigorous coupled wave analysis (RCWA) calculations, are used to guide the fabrication of sub-wavelength scale nano-textures designed to impart AR, HR, and filtering functions. The software allows the propagation of light through a user defined three-dimensional surface texture composed of multiple structured and uniform materials. By solving Maxwell’s equations at each material interface, the model predicts the spectral reflectance and transmittance, accounting for arbitrary polarization states and light incident angles. Measured data for the optical constants of a library of materials is included and regularly updated and augmented. Model predictions have proven to be a good match to measured ARMs, polarizer, and HR microstructure prototype performance.



Figures 2 illustrates the use of SEM to measure the dimensions of the features in a fabricated ARMs texture that can in turn be input to the design software to determine how well the measured performance matches the model prediction. Three types of ARMs textures designed for peak performance at laser wavelengths in the near IR are shown etched in the surface of sapphire windows. A sketch of the texture profile is given below each set of images. The SWS-type ARMs surface of sapphire window S117 shown on the left consists of an array of round mesas with nearly vertical sidewalls etched about 160nm high on a 385nm pitch grid. SWS textures can yield extremely low reflectivity at a design wavelength, but this peak performance wavelength depends critically on the feature fill factor and etch depth, with fill factor being the most difficult to control with current fabrication methods. This issue drives the development of Motheys and Hybrid type ARMs textures that can achieve similar AR performance with increased fabrication tolerance and wider bandwidth, but at the expense of greater etch depth and requiring tapered or even non-linear profiles^[10]. Blunt tip cone-like features approaching the Motheys ARMs design with high fill factor are etched about 300nm deep in the surface of sample S114 shown by the center images. The tapered sidewall high fill factor mesas etched in sample S68B on the right, show an intermediate or Hybrid design between Motheys and SWS type ARMs.

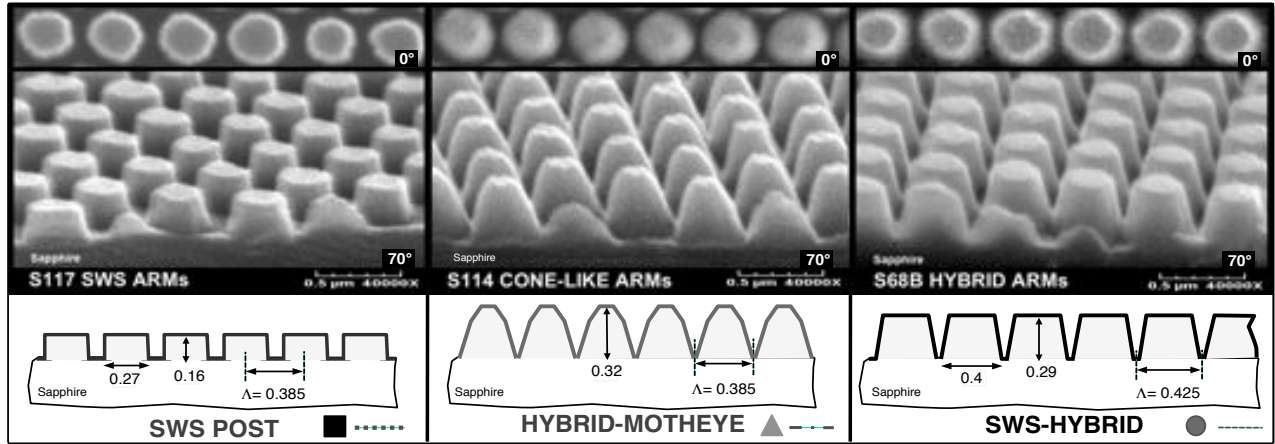


Figure 2: Overhead (0°) and elevation (70°) SEM images along with measured cross section dimensions of ARMs in sapphire.

Figure 3 shows the measured normal incidence spectral reflection over the near IR of the three ARMs textured sapphire windows of Figure 2 matched to the reflection of modeled ARMs textures predicted by the RCWA calculation. A log scale is used to detail the low reflectivity achieved and to better illustrate the correspondence of the measured (solid lines with markers) and modeled (dotted and dashed lines) data. A reflectivity minimum of just 0.02% is recorded near the 780nm pump laser wavelength of a rubidium vapor DPAL for SWS ARMs in sapphire sample S117 (black square markers). The Hybrid-Motheye cones of sample S114 (grey open triangle markers) reduce reflections to the 0.03% level at the high power laser diode wavelength of 940nm used to pump ytterbium YAG gain media. And a level approaching the spectrometer noise floor at 0.015% is found for the Hybrid-SWS mesas etched in sapphire sample S68B (dark gray circle markers). To achieve the close match of the measured data illustrated in Figure 3, the feature dimensions entered to the simulation such as fill factor and height were varied by as much as 25% relative to the dimensions measured by SEM analysis. After accounting for a 15% error in measuring the feature dimensions by SEM, such a variation is not beyond the range of practicality for design to match fabrication results.

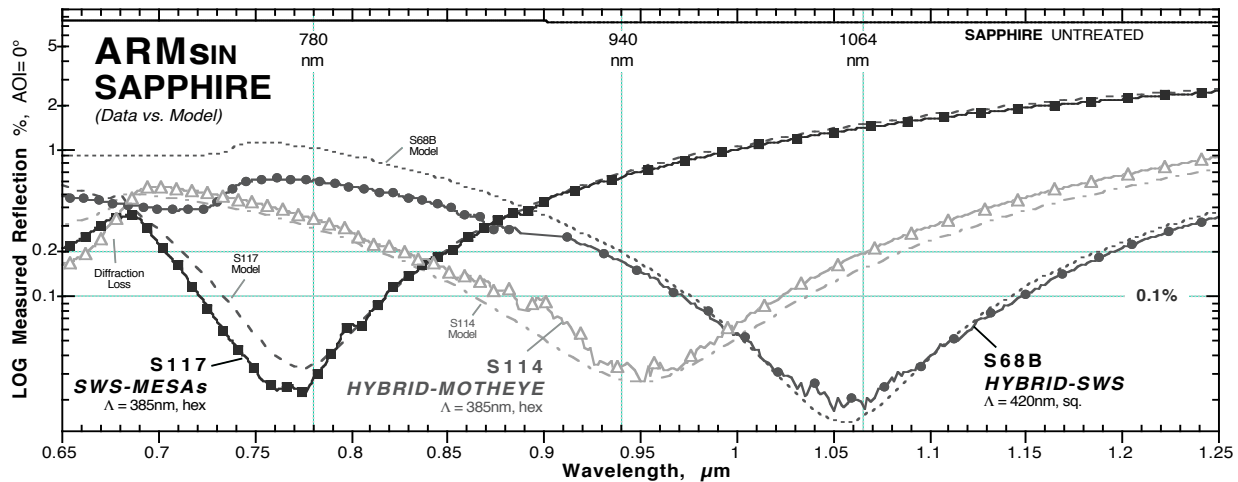


Figure 3: Plot of the measured reflection of the Figure 2 ARMs textured sapphire windows compared with the model prediction.

3.0 ARMs FABRICATION, MEASURED PERFORMANCE, AND LASER DAMAGE TESTING

In this work non-periodic Random ARMs textures and periodic Motheye- and SWS-type ARMs textures were fabricated in planar windows of eight relevant laser materials, namely fused silica, Schott N-BK7 glass, Schott Borofloat 33 glass, single crystal sapphire, neodymium-doped YAG, and polycrystalline magnesium aluminate spinel ($MgAl_2O_4$, SPINEL). Random ARMs textures were fabricated in fused silica and glass windows using an efficient, proprietary, one-step plasma etch process that has the potential for low cost volume manufacturing.^[15-17] Periodic Motheye and SWS ARMs textures were fabricated in a two stage holographic lithography^[23] and plasma etch process that has been described in prior publications.^[10,11,18,19]

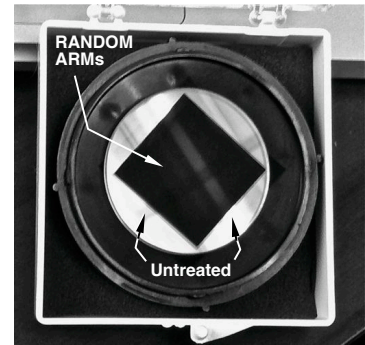
Prior to ARMs texture fabrication, each material sample is screened for polishing defects and then aggressively cleaned using soaps, solvents, and acids specific for each material type. The transmission and reflection of each sample was measured using two grating-based spectrometers to cover the wavelength range of from 0.4 μ m to 1.7 μ m. These spectrometers employ multi-mode fiber optic cables equipped with collimating lenses to transmit a broad-band tungsten-halogen light source through each sample, and to return the transmitted light to the spectrometer input. A single bifurcated fiber cable is used to send and receive a collimated white light beam during reflectance measurements. To isolate reflections from just one surface, a backside absorber plate is constructed for each material consisting of a polished slab roughened and painted black on one side. The part under test is then placed on the polished surface of the absorber and index matching fluids are used to couple the transmitted light into the black paint (decalin, $n=1.48$ for fused silica and borofloat glass, xylene, $n=1.51$ for N-BK7 glass, diiodomethane, $n=1.72$ for sapphire and SPINEL, and a Cargille $n=1.8$ fluid for Nd:YAG). Send and receive fibers can be oriented at any angle ($\pm 70^\circ$) with respect to the sample plane, but in most cases normal incidence reflectance and transmission data was collected for this work.

3.1. Random ARMs in Fused Silica, Quartz, Schott N-BK7 and Borofloat 33 glass.

Fused silica glass material is widely utilized for components in HEL systems due to its durability and low absorption over the UV through NIR spectral range. The borosilicate glass BK7 originated by Schott, is used for high quality optics and laser windows in systems that operate on visible through NIR wavelengths due to its highly controlled refractive index, low internal defect level, and moderate cost. Although not yet widely applied in laser applications, the sheet glass produced by Schott known as Borofloat 33, has the potential to provide a low cost replacement for fused silica based windows and filters in NIR applications such as telecommunications, medical devices, and industrial lasers.

The exceptional bandwidth and performance of Random ARMs in fused silica is illustrated by the image on the right where Random ARMs textures have been fabricated in the central square area of a 38mm diameter window, effectively eliminating the image of an overhead light fixture readily observed reflecting from the untreated areas around the window perimeter.

Random ARMs textures, tailored in density and depth for a specific laser application, were fabricated in fused silica, quartz, N-BK7, and borofloat glass windows and subjected to standardized pulsed laser damage testing at wavelengths of 532nm, 694nm, 800nm, 1064nm, and 1538nm.



3.1.1 **532nm**, 10ns Pulsed LiDT Testing: ARMs in Fused Silica, BK7, Borofloat Glass



The Survivability/Lethality Analysis Directorate (SLAD) of the Army Research Laboratory (ARL) at White Sands Missile Range New Mexico, operates a 532nm wavelength pulsed laser system that includes a liquid dye cell. This cell is constructed from fused silica windows containing a solvent-borne chemical through which the beam must travel. ARL could not operate their system at the high energies desired due to the short lifetimes of the thin-film ARCs available for the fused silica dye cell windows, a problem further aggravated by degradation of AR coating materials when in contact with the dye cell chemicals. ARL wanted at least a 2x improvement in the survivability of the fused silica windows, and were thus motivated to conduct comparison testing of Random ARMs treated fused silica, untreated fused silica, and two types of thin-film ARCs supplied by CVI-Melles Griot. ARL purchased four UV grade fused silica windows from CVI (each 1.5-inch round, 3.2mm thick, polished to 10-5 scratch-dig, $\lambda/10$ flatness, CVI # PW1-1512-UV) that were subsequently textured with Random ARMs in one surface of two samples, and both surfaces of another two samples. ARL also purchased two fused silica windows with the same polish specification that were coated on both sides with an ion beam sputtered (IBS) dual-band TFARC for one sample (CVI # IF-1525-UV-425-675), and a single layer magnesium fluoride (MgF_2) TFARC on the second sample (CVI # PW1-1512-SLMF-400-700) chosen not for its performance but for its chemical resistance to the dye. The spectral reflection and transmission from each of the six samples along with a seventh uncoated – or untreated, as-received sample – were measured over the wavelength range of 400-1000nm. A log scale plot of the single surface normal incidence ($AOI=0^\circ$) reflection values are given in Figure 4 above where the untreated fused silica sample is plotted as the heavy solid black line, the single layer MgF_2 coated sample reflection is plotted as the thin solid black line, the IBS TFARC window reflection is plotted as the thick solid gray line, and the Random ARMs textured sample reflection curves are given as the dashed black curve (AR textured both sides) and the dotted black curve (one side AR texture). Note the peak AR performance at short wavelengths and the monotonic increase for longer wavelengths that is typical of the graded index function produced by both Random and Motheye ARMs treated surfaces. At the damage test wavelength of 532nm the Random ARMs sample reflectivity is below 0.2%.

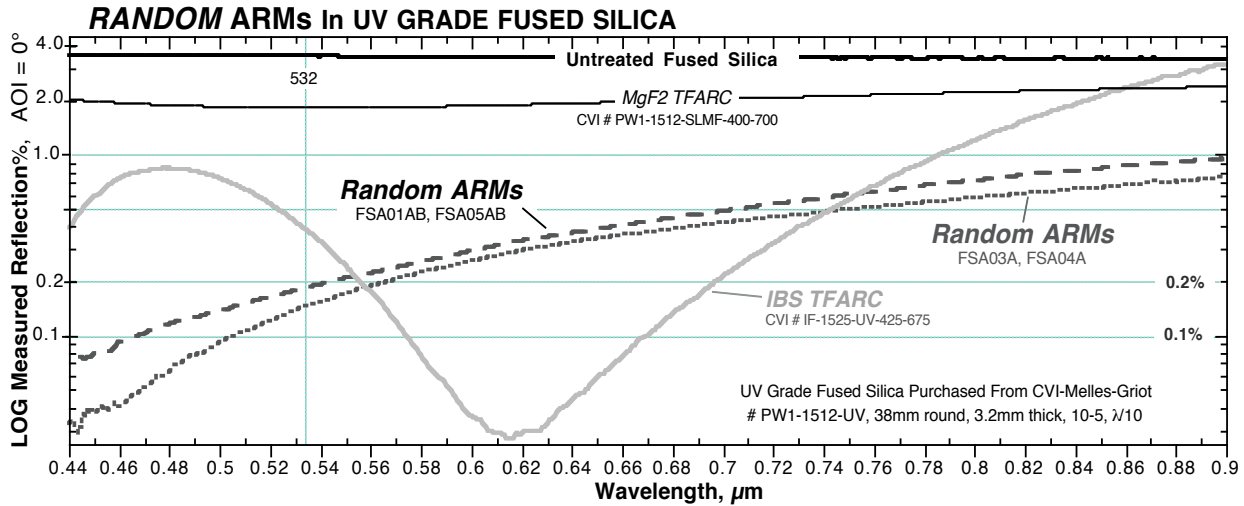


Figure 4: Measured reflection (log scale) of untreated, ARMs treated, & thin-film AR coated fused silica – 532nm LiDT tests.

ARL conducted both 1-on-1 and accumulated power until damage tests on all seven samples that were based on the ISO 11254-2 standard. A Quantel model YG981-E doubled Nd:YAG laser was employed operating with a pulse width of 10ns (measured at full width half maximum, FWHM), a pulse repetition rate of 15Hz, a slightly asymmetric Gaussian beam focused on the sample surface with a $1/e^2$ diameter of 290µm (monitored in real time and corrected to TEM₀₀ for the fluence calculation). A single energy level was delivered to each exposure site with 150 pulses (shots) delivered at each site – a 10 second exposure duration. Each sample was rotated several beam diameters between exposures to avoid any debris from damage at the neighboring sites. The pulse energy was increased at each new site until permanent surface damage was observed by the naked eye. A least four damage sites were produced on each sample. The observation of damage without increased magnification or Nomarski is non-standard, but was applied in a consistent manner. This damage criteria most likely leads to higher reported thresholds due to missed smaller scale damage, but is mitigated by the fact that normally disregarded back surface damage was included in the count.

The energy per square centimeter, or fluence, needed to damage a surface site is given by the bar chart of Figure 5 with the multiple damage sites represented by individual bars grouped together by sample type. Nine sites with an average damage threshold of 9.8 J/cm² were produced on the untreated fused silica window as indicated by the solid grey bars. Four damage sites were produced on each of the single and double sided Random ARMs treated fused silica windows (black and white textured bars) where the average damage threshold was extremely high ranging from a low of 37 J/cm² to a high of 52.7 J/cm². This level is three to five time higher than the 13.5 J/cm² level found as the average of 8 damage sites produced on the IBS TFARC sample (grey and black tipped white bars). The damage threshold of Random ARMs was also found to be 1.5 to 2 times higher than the low performing single layer MgF₂ TFARC sample shown as the grey tipped white bars.

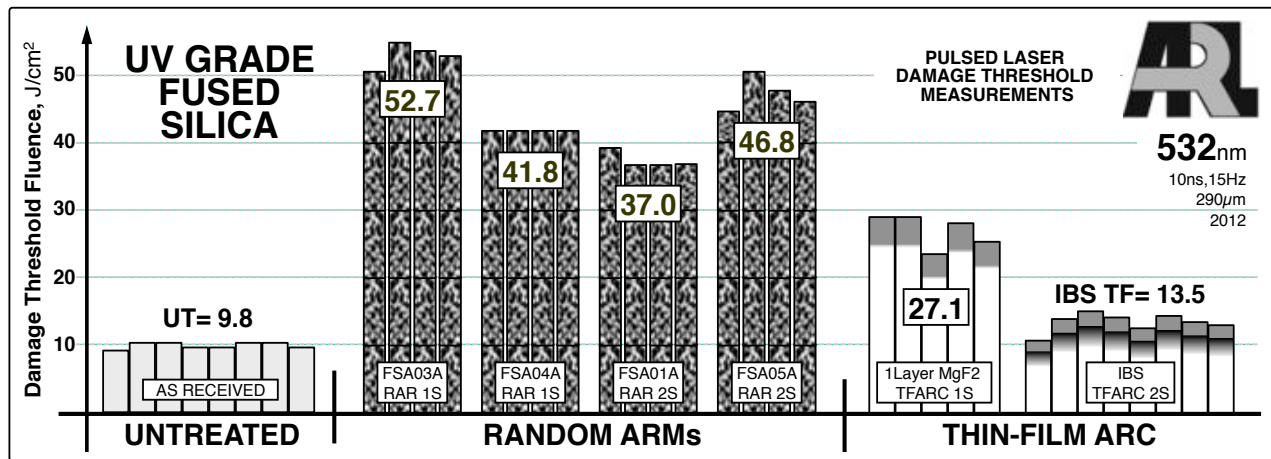


Figure 5: Bar chart showing the LiDT of untreated, ARMs treated, and thin-film coated UV grade fused silica windows at 532nm.

In order to confirm the ARL SLAD results and to better compare the threshold values with those specified for catalog optics and published in the literature, s-on-1 testing was conducted using the certified services of Quantel USA in Bozeman, Montana. In addition to the same untreated, Random ARMs-treated, and IBS TFARC fused silica windows acquired from CVI, the standardized tests were expanded to include inexpensive Corning 7980 fused silica with a simple commercial polish, as well as two other glass materials, namely Schott N-BK7 with a simple commercial polish and borofloat 33 as manufactured. Recently, the Random ARMs fabrication process has been adapted for BK7 glass where AR performance over the visible to NIR wavelength range is good but not yet up to the high level attained with Random ARMs in fused silica and borofloat glass. Figure 6 shows SEM images of the dense Random ARMs texture etched in the surface of a BK7 glass window.

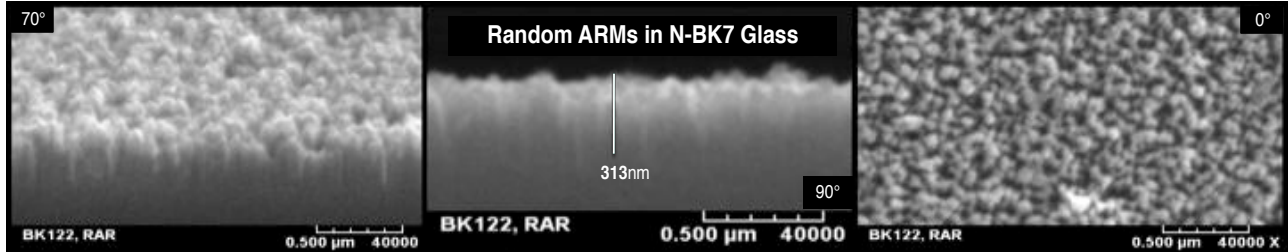


Figure 6: Elevation (70°), profile (90°), and overhead (0°) SEM images of a 0.3µm deep Random ARMs texture in BK7 glass.

Nineteen samples were submitted to Quantel for s-on-1 testing at 532nm. The sample matrix consisted of 2 untreated, 2 Random ARMs treated, and 2 IBS thin-film AR coated UV grade fused silica windows purchased from CVI, 2 untreated and 2 Random ARMs treated Corning 7980 fused silica windows, 2 untreated and 3 Random ARMs treated Schott N-BK7 windows, and 2 untreated and 2 Random ARMs treated Schott borofloat 33 windows. Figure 7 shows the measured reflection of the test samples over the wavelength range of 440-900nm. Of note is the wide-band performance (0.09% average 400-750nm) and deep reflectance minimum below 0.03% found near the 532nm damage test wavelength for the Random ARMs treated Schott borofloat 33 windows (dotted black curve).

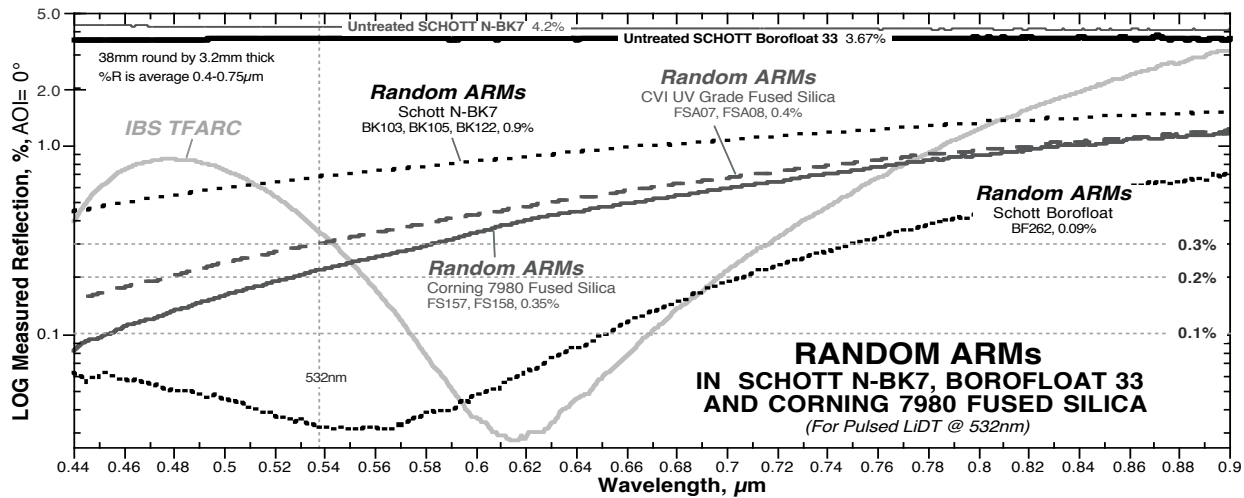


Figure 7: Measured reflection of untreated, ARMs treated, & thin-film AR coated windows for the Quantel 532nm LiDT tests.

Quantel's s-on-1 test adheres to the ISO 11254 standard and involves exposing 100 or more discrete surface sites on a sample to as many as 10 calibrated fluence levels below and above the damage threshold, repeating each fluence level at 10 or more sites. The result is then expressed as a damage frequency as a function of fluence level with a linear fit to the data determining the threshold. The specific test configuration was a 532nm wavelength, 10ns pulse width (FWHM), 20Hz pulse repetition rate, 370µm spot diameter ($1/e^2$), TEM₀₀, linear polarization, AOI=0°, 80-120 sites, 200 shots per site. The damage criteria was observation of permanent surface damage under 150X magnification using Nomarski polarized imaging. It is common in fused silica and other glasses under test to observe large scale back surface damage, or blow outs like that shown in the image on the right. Often this backside damage occurs without damage to the expose surface and is therefore not included in the damage site count. In fact when such backside damage occurs the pulsing is stopped to avoid propagating the damage over a larger area that might encroach upon the adjacent exposure sites.

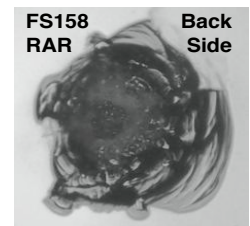


Figure 8 gives a scatter plot of the damage frequency data as a function of the fluence level for the 10 fused silica windows tested. As with the ARL testing, the damage threshold of the Random ARMs treated fused silica windows (solid black and grey lines and triangles) is found to be 3 to 5 times higher than the IBS TFARC samples (black squares, dashed line). Unlike the ARL testing, the untreated fused silica windows (open crosses, dotted lines) showed high thresholds that are comparable to the Random ARMs treated windows and consistent with previous damage testing results at multiple wavelengths. (The cause of the low ARL measurement is unknown at this time). As expected from numerous literature references and prior experience, the untreated fused silica windows with the high level of surface polish (10-5 scratch-dig, $\lambda/10$) exhibited a damage threshold 30% higher than the inexpensive fused silica with a simple commercial polish (80-50 scratch-dig, $2-5\lambda$). However, the data for the Random ARMs treated windows suggests that a lower level of initial surface polish can be partially mitigated by the Random ARMs fabrication process which consumes a portion of the surface material and possibly removes or diminishes residual sub-surface polishing damage.

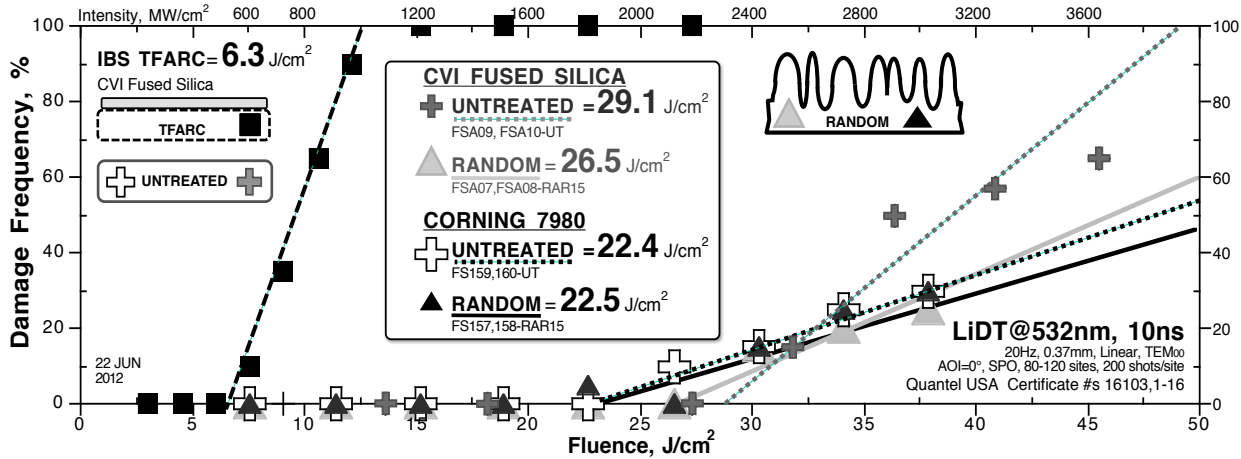


Figure 8: Damage frequency as a function of fluence level for fused silica windows at 532nm, Quantel data.

The threshold of 6.3 J/cm^2 at 532nm, 10ns pulse width for the CVI IBS TFARC is close to the 5 J/cm^2 damage threshold specified in the catalog for a 20ns pulse. Edmund Optics lists the damage threshold of its V-coatings at 10 J/cm^2 at 532nm, 10ns pulse. Random ARMs textures then can be expected to exhibit a damage resistance at least 2.5 times higher than the best performing commercial TFARCs.

Figure 9 shows a bar chart comparing the damage thresholds for all 19 windows tested. Schott BK7 glass exhibits a damage resistance comparable to the fused silica results for both the untreated (white bars) and Random ARMs treated windows (black and white textured bars). Threshold values in the range of 26 to 34 J/cm^2 combined with reduced cost should open up further high power laser applications for the less expensive BK7 glass material. Unexpectedly, the damage threshold for borofloat glass at 532nm is quite low compared to the high values found at longer wavelengths (694, 800, 1064, & 1538nm). This may be due to absorption in the bulk as the thresholds for both the untreated surfaces and the ARMs treated surfaces are comparable.

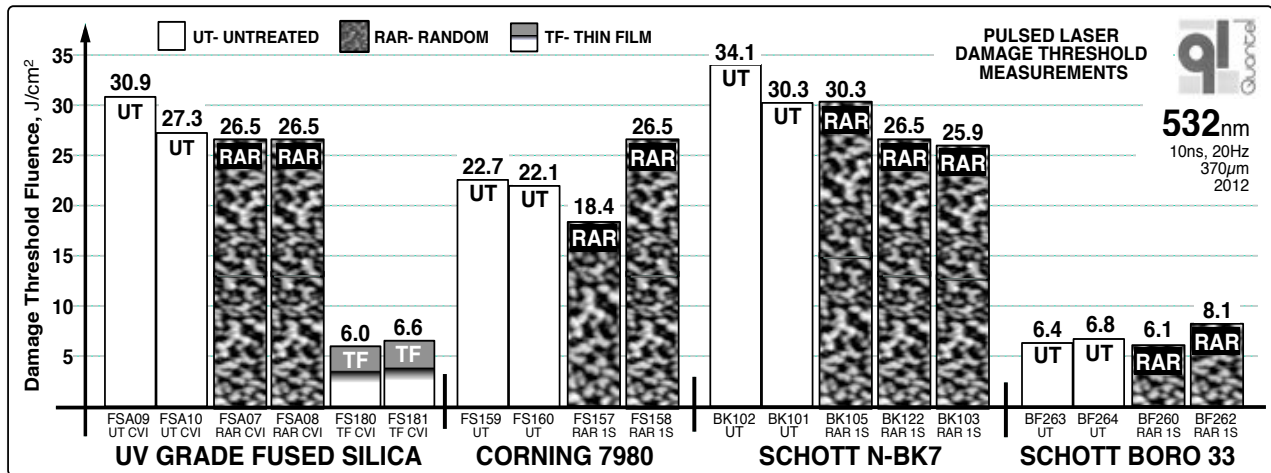


Figure 9: Bar chart showing the LiDT of ARMs in fused silica, BK7, and borofloat windows at 532nm.

SEM imaging of multiple damage sites was made in an effort to understand the nature and differences of the laser induced damage for each material type. Although large area damage was obvious and readily assigned to fluence levels producing a 100% damage frequency, it proved very difficult to image smaller area damage sites produced by energy levels near the threshold. This may be due to the damage sites nearest the threshold being slight refractive index distortions readily observed in the polarized light (Nomarski) used during the test, but with little or no surface relief that can be imaged by SEM. Figure 10 shows 45° elevation views at two magnification levels of two different damage sites.

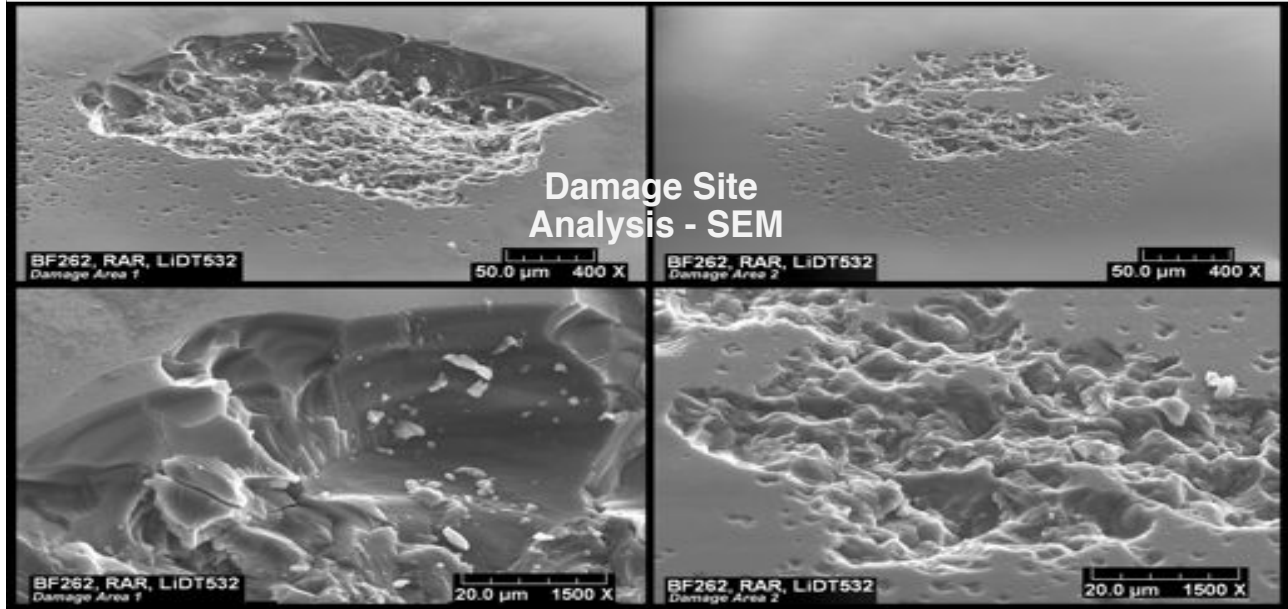


Figure 10: Elevation (45°) views at two magnifications of damage sites created in borofloat glass during the 532nm testing.

3.1.2 **694nm, 26ns Pulsed LiDT Testing: ARMs in Fused Silica, Borofloat Glass**

With the great number of medical applications operating ruby ($\text{Cr:Al}_2\text{O}_3$, 694nm) and alexandrite ($\text{Cr:BeAl}_2\text{O}_4$, 755nm) lasers with increasing power levels, the need to enhance the survivability of the optics in these lasers is driving the development of higher damage resistance thin-film coatings. Significant improvements to damage resistance can be made by replacing AR, HR, and filter thin-film coatings with AR, HR, and filter microstructures built directly in the fused silica optics, fiber delivery systems, and laser gain media. In particular the high performance and wide bandwidth of Random ARMs textures could significantly increase the reliability of medical laser systems that combine multiple wavelengths ranging from 532nm to 1320nm.

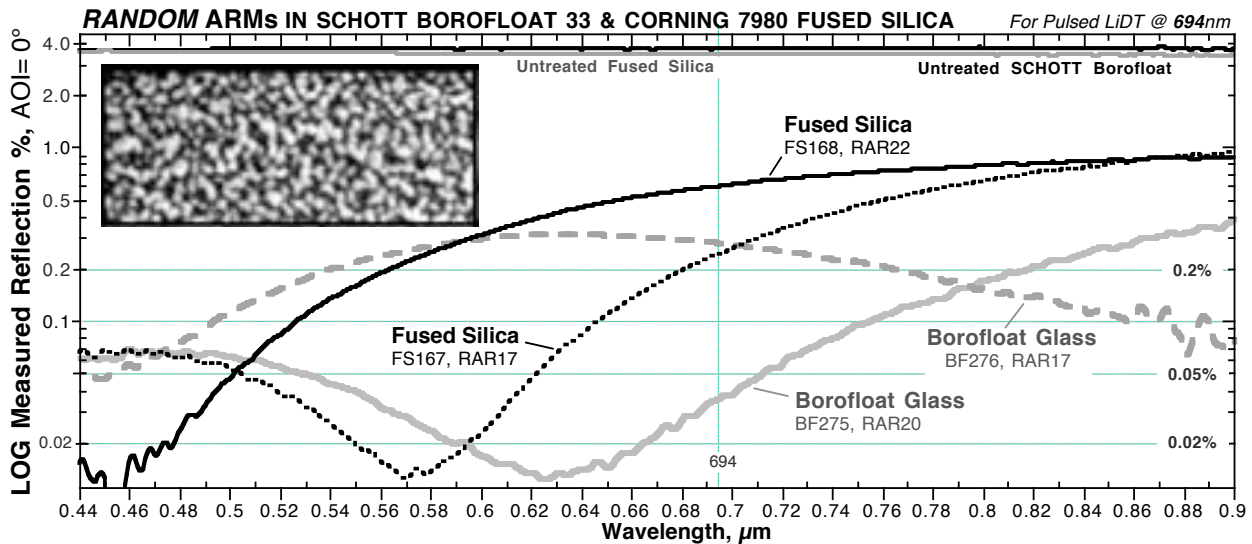


Figure 11: LOG plot of the measured reflection from ARMs treated fused silica and glass windows prior to 694nm LiDT testing.

To further qualify ARMs for medical laser optics, Random ARMs textures were fabricated in Corning 7980 fused silica and Schott borofloat 33 glass, and submitted to Quantel for pulsed laser damage testing using their ruby laser system operating at a wavelength of 694nm. Figure 11 above shows the measured spectral reflection from the four ARMs-treated test samples over the wavelength range of from 0.44 to 0.9µm, where the density and depth of the Random ARMs texture was varied to observe the impact on damage resistance at 694nm. The two fused silica samples (solid and dotted black curves) showed a reflectivity of 0.7% and 0.25% at 694nm, while the two borofloat glass samples (solid and dashed grey curves) showed even lower reflection with values of 0.25% and 0.03%. (An overhead SEM image of the Random ARMs texture in borofloat glass taken at 40,000X magnification is inset in the figure).

Quantel conducted standardized s-on-1 damage testing on the four ARMs treated samples as well as four untreated windows (2 fused silica & 2 borofloat) with surfaces cleaned in solvents and acids only - no additional surface polishing. The ruby laser was operated with a 26ns pulse width (FWHM), 0.2Hz repetition rate, linear polarization, TEM₀₀ spatial mode. The beam was directed at normal incidence to the test surface and focused to a monitored and calibrated spot size of 350µm (1/e²). Up to 9 energy levels were delivered to 90 sites with each site receiving only 20 pulses due to the long (5 seconds) pulse repetition time (about 3 hours of test time per sample!).

Figure 12 shows the test results as a plot of the damage frequency verses fluence level for all 8 samples. The raw data showed little variation between like variants and therefore the data from the two samples of each variant was averaged to generate the four linear curves shown in the figure. Very high damage thresholds of 87 J/cm² and 64.5 J/cm² for the untreated (open crosses, dotted black curve) and Random ARMs treated (solid black triangles, black curve) fused silica respectively, are found, values easily 3 times higher than those specified for commercial thin-film AR coatings. It is expected that further refinement of the Random ARMs fabrication, cleaning and surface preparation processes can yield damage thresholds that are consistently equivalent to untreated surfaces. Damage thresholds for the Schott borofloat 33 glass were found in the 31-33 J/cm² range for both untreated (solid gray crosses, dotted gray line) and Random ARMs treated (solid gray triangles, solid gray line), values at least 50% higher than TFARCs, about half the fused silica levels.

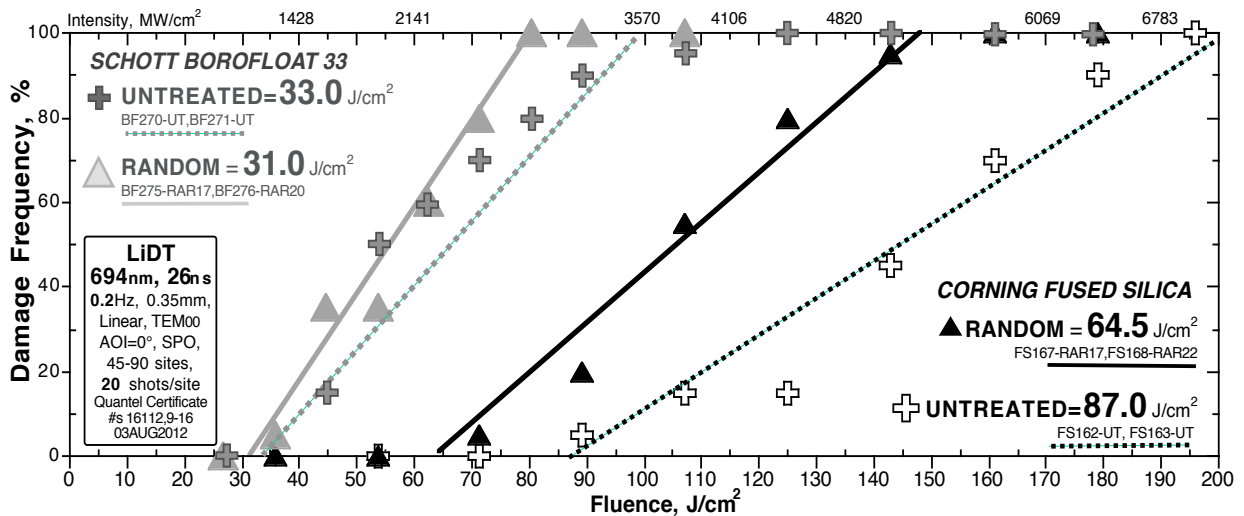


Figure 12: Damage frequency vs. fluence for untreated and Random ARMs treated fused silica and glass windows at 694nm.

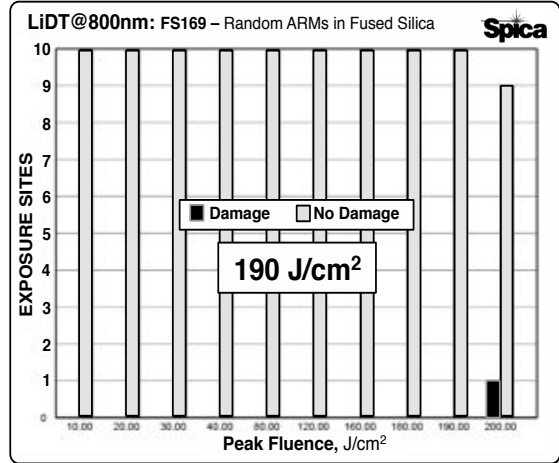
3.1.3 800nm, 10ns Pulsed LiDT Testing: ARMs in Fused Silica, Borofloat Glass

High power laser diodes operating at 808nm have a primary application as optical pumps for Nd:YAG solid state lasers. Many high power laser diodes operating at a 780nm wavelength can be combined to power scale DPAL systems to the multi-kilowatt level. The thin-film coatings used for the optical fibers, windows, and lenses needed to manipulate high fluence levels, have exhibited such low damage resistance that their use is often avoided in favor of power limiting methods such as angle cutting fiber facets and utilizing a Brewster angle configuration. The durability and extreme AR performance of Random ARMs textures in fused silica offers the potential to eliminate such limitations and significantly increase the survivability of fused silica components in DPAL and solid state laser systems.

Random ARMs textures were fabricated in Corning 7980 fused silica and Schott borofloat 33 glass, and submitted to SPICA Technologies of New Hampshire for pulsed laser damage testing using their Ti:sapphire laser system tuned to a wavelength of 800nm. Four untreated and four ARMs-treated test samples were cleaned and prepared using the same methods as described above for the 532nm and 694nm testing. The spectral reflection of each sample was measured to

be substantially similar to the data shown in Figure 11 above with the ARMs treated borofloat sample reflectivity recorded below 0.15% at 800nm, and the fused silica sample reflectivity recorded at 0.6% at 800nm. (Note that the fused silica Random ARMs samples were originally produced for the 532nm damage tests where they exhibit a reflectivity below 0.05%. Much lower reflectivity in the NIR is demonstrated for Random ARMs in fused silica as part of the next section on 1064nm testing.)

SPICA conducted s-on-1 damage testing based on the ISO 11254 standard on the eight samples with the Ti:sapphire laser configured for a 10ns pulse width (FWHM) and a 10Hz pulse repetition rate, producing a linearly polarized beam running multiple longitudinal modes with a TEM₀₀ spatial mode. The beam was directed at normal incidence to the test surface and focused to a monitored and calibrated spot size of 139µm (1/e²), later reduced to 62µm due to the power limitations of the system. Up to 10 energy levels were delivered to 80-120 sites with each site receiving 200 pulses for an exposure duration of 20 seconds per site. The criteria for damage is observation of increased scattering of a red helium-neon gas laser beam illuminating the test site combined with a permanent surface change observed by visual inspection through a microscope configured for 150X magnification and Nomarski polarized imaging. SPICA returns tabular data and a histogram chart for each sample, one of which is shown above on the right. As opposed to making a linear fit to the damage frequency verses fluence data, SPICA defines the damage threshold by the “least fluence failure” method, placing the threshold at the energy level where no damage is observed at any site, just below the energy level where damage is first recorded. If the energy level step size near the threshold is small, then this method and the Quantel linear fit method are essentially equivalent.



A bar chart comparing the damage thresholds for all 8 windows is shown in Figure 13 on the right. Exceptionally high damage thresholds in the range of 180 J/cm² are found for both material types and for both the untreated and the Random ARMs treated samples. SPICA had great difficulty finding an energy setting that would yield damage at a reasonable spot size and was forced to drop the spot size down to where the spot diameter measurement error may be a factor in producing such high damage fluence values. In addition, most damage thresholds were found with just 1 damage site out of 10 exposed to power levels near the Ti:sapphire laser maximum – as illustrated by the histogram plot above. In any case the relative values for untreated and ARMs treated samples indicate that the Random ARMs etching process may have a positive effect on the damage

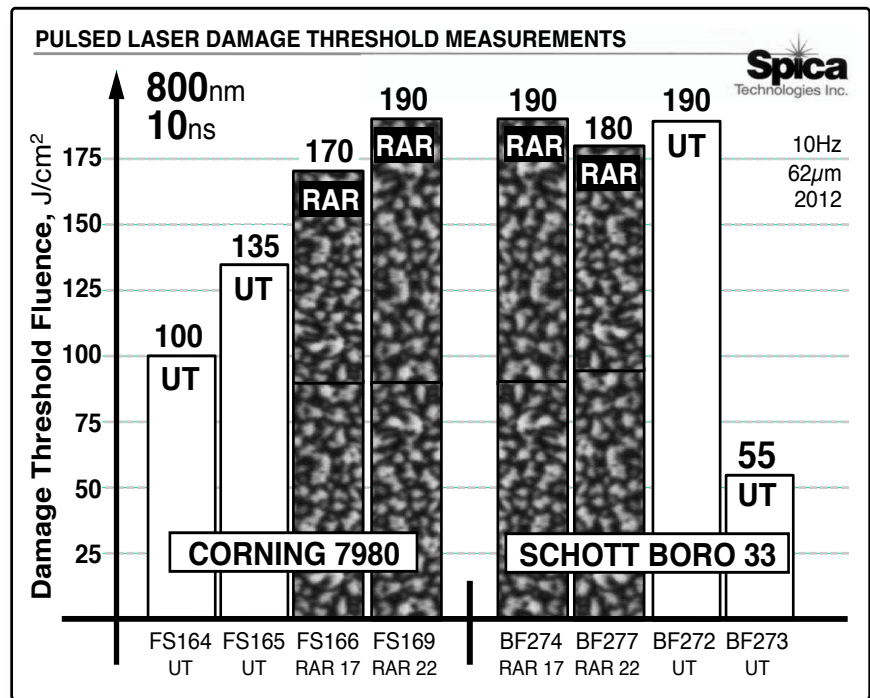


Figure 13: Bar chart giving the LiDT of untreated (UT) and Random ARMs treated (RAR) fused silica and borofloat windows at 800nm.

threshold by removing residual subsurface damage or surface contaminants. Note that the damage threshold for Schott borofloat glass has increased at this longer wavelength to match the fused silica levels, suggesting that its greatest utility may be as low cost windows and filter substrates operating with NIR laser light.

3.1.4 **1064nm, 10ns Pulsed LiDT Testing: ARMs in Fused Silica and Single Crystal Quartz**

With the great number of applications for the solid state laser based on Nd:YAG gain media operating at a wavelength of 1064nm, many catalog optics companies now list a pulsed laser damage threshold for their narrow-band TFARCs (“V-coat”) deposited on UV grade fused silica or Schott N-BK7. A standard has emerged for s-on-1 testing at 1064nm with a 10ns pulse width and a 20Hz pulse repetition rate. The catalog optics companies Thor Labs, Edmund Optics, and Newport, all specify a threshold of 10 J/cm², 1064nm, 10ns for V-coat TFARCs on fused silica laser line windows^[24-26]. CVI-Melles Griot (now IDEX) specifies 15 J/cm² for their V-coat but at a 20ns pulse width where the longer pulse width is expected to yield higher damage thresholds^[27]. Only a few of the many companies advertising high damage thin-film AR coating services have specified the actual threshold value. These include Rocky Mountain Instrument (RMI) that specifies 10 J/cm² at 1064nm, 10ns^[28], and Precision Photonics specifying >10 J/cm² at 1064nm, 10ns for a TFARC on a beam splitter optic^[29].

In this work, the pulsed LiDT of ARMs treated fused silica and single crystal quartz was measured by Quantel using their 1064nm, 10ns, 20Hz Nd:YAG laser test-bed. (The birefringent quartz windows, each 1-inch round by 1mm thick, were purchased from Boston Piezo Optics in Bellingham Mass, z-cut to present a uniform refractive index in the plane of the window, and chemically polished to a 40-20 scratch-dig, 5 wave flatness.) A total of 11 planar windows were tested that included untreated (as polished) samples and both non-periodic Random ARMs, and periodic SWS ARMs textures etched in both material types. Figure 14 shows the measured spectral reflection of all the samples tested over the NIR wavelength range where a vertical dashed line marks the 1064nm wavelength. Overhead SEM images at a magnification of 20,000X are given in the figure showing Random ARMs in quartz (top) consisting of a dense carpet like texture compared to an SWS ARMs texture in quartz (bottom) consisting of a hexagonal array of holes with a grid spacing of 520nm and a depth of about 250nm. For the eight ARMs treated samples, the normal incidence surface reflection has been reduced below 0.3% at 1064nm, reaching 0.1% for one of the Random ARMs treated quartz windows (open circles, grey curve).

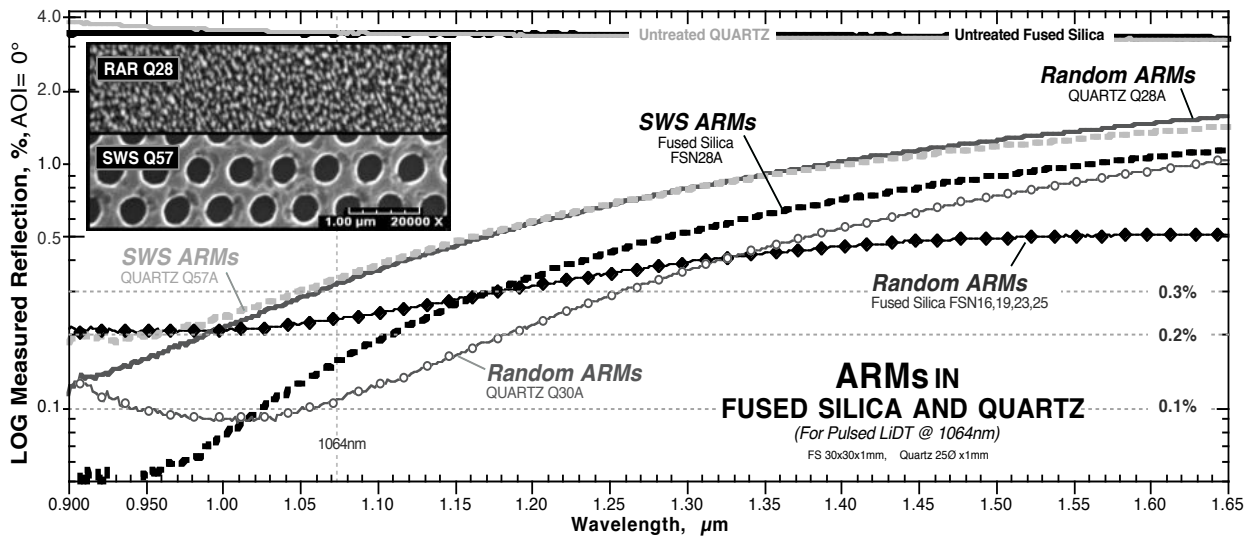


Figure 14. Measured NIR spectral reflection of Random & SWS ARMs in quartz & fused silica windows, for 1064nm tests.

Figure 15 gives a bar chart summarizing the results of the Quantel 1064nm, 10ns LiDT testing (500μm spot size, normal incidence, >100 sites, 200 shots/site). High damage thresholds are again found for Random ARMs in fused silica (black and white bars labeled RAR) averaging 32.6 J/cm² for the four windows tested, a level more than 3 times greater than the TFARC thresholds described above. These untreated (white bars labeled UT) and Random ARMs treated values are consistent with the single data points collected by Quantel in 2007 using a longer 20ns pulse width (shown on the right side of Figure 15). The damage threshold for the SWS ARMs texture in fused silica (graded gray bar labeled SWS) is 24.6 J/cm², a bit lower than the Random ARMs samples likely due to non-uniformities and defects in the period array. Increased defect levels due to handling may also explain the slightly lower thresholds found for two of the four Random ARMs treated windows that were processed with ARMs in both surfaces. Threshold levels for the ARMs treated quartz windows were generally lower than the fused silica windows, but still averaged 24.6 J/cm², about 2.5 times greater than TFARCs. There is more variability in the quartz data likely due to a combination of handling defects, material differences, surface preparation, and AR performance.

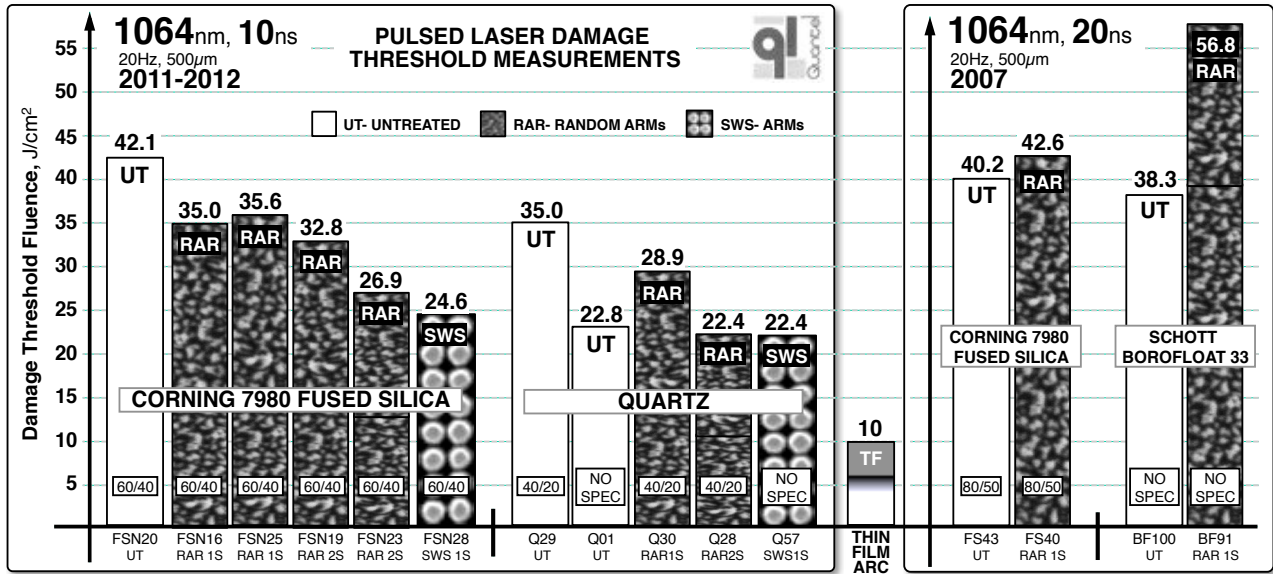


Figure 15: Bar chart showing the LiDT of ARMs in fused silica, quartz, and borofloat windows at 1064nm.

3.1.5 1538nm, 14ns Pulsed LiDT Testing: ARMs in Fused Silica

As power levels produced by fiber lasers and transmitted by fiber optic communications systems increases, the survivability of TFARCs on fused silica materials in such systems is becoming marginal. ARMs textures etched into fiber facets and optical devices offer increased transmission combined with a significant increase in system reliability. To illustrate the pulsed laser damage resistance of ARMs in fused silica at telecom wavelengths, one of the Random ARMs textured fused silica windows prepared for the 1064nm damage testing described above, was submitted to Quantel for s-on-1 testing at 1538nm along with an untreated window, and a window with SWS ARMs etched in one surface. The SWS ARMs textured window was also prepared for the 1064nm testing, consisting of a hexagonal array of holes on a 525nm pitch, but etched deeper to shift the peak performance to a longer wavelength closer to 1538nm. The measured spectral reflection of these samples is shown in the plot on the left in Figure 16 along with data from fused silica windows tested at 1538nm by Quantel in 2007. Note that the AR performance was not set to peak at 1538nm, but rather to match the performance of the 2007 samples. Results of the Quantel testing are shown in the bar chart on the right of Figure 16, where the test parameters were; 1538nm wavelength, 14ns pulse duration, 20Hz repetition rate, 0.3mm spot size, TEM₀₀, multiple longitudinal modes, linear polarization, 100 sites, 200 shots/site. As with the 2007 results and consistent with the 1064nm results, high damage thresholds are found for the ARMs treated samples, values that are comparable to the untreated material and likely 3 times greater than TFARCs. The difference in the general threshold level between the 2007 and 2012 samples is likely due to absorption in the different grades of fused silica.

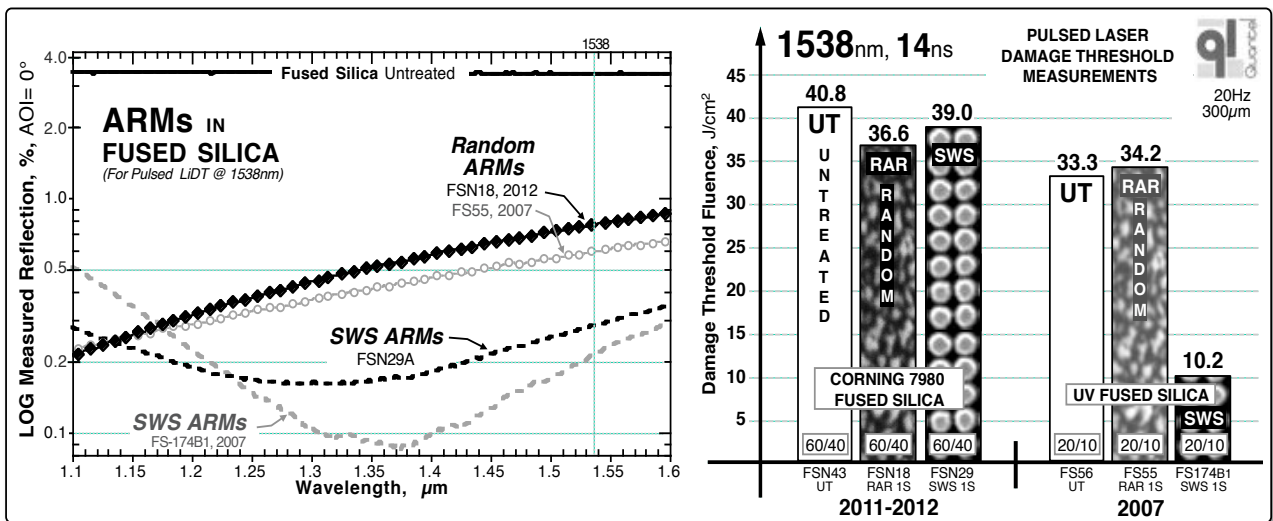


Figure 16. Measured reflection of ARMs in fused silica (left) and the results of pulsed LiDT testing at 1538nm (right).

3.2. ARMs in Sapphire.

The gain medium in a potentially kilowatt or even megawatt class HEL known as a diode pumped alkali laser, or DPAL, is a vapor of rubidium, cesium, or potassium contained within a cell made of an optically transparent material, typically glass or quartz. Pump light is absorbed by the vapor and re-emitted and subsequently resonated by the laser cavity optics. Alkali vapor chemically attacks and damages the typical glass or quartz cell materials as well as the necessary AR treatment currently based on depositing thin-film ARC materials. Deposits of alkali hydrates and carbon can also be formed. Both the chemical erosion and deposits lead to very short lifetimes at high power levels. The solution is to replace thin-film coatings and cell windows with ARMs textures etched in the chemically resistant material sapphire. Sapphire also has high mechanical strength, is easily cleaned, and has high thermal conductivity.

On a current contract through the High Energy Laser Joint Technology Office (HEL-JTO), the concept of utilizing the natural chemical resistance of sapphire combined with the high performance of ARMs to enhance the survivability of DPAL gas cell windows is being pursued. Periodic SWS-type ARMs textures were designed and then fabricated using interference lithography to originate the array of sub-wavelength sized features in a hard mask material that was subsequently employed to transfer the texture into the surface of sapphire windows using a proprietary reactive ion etch process. Multiple samples of ARMs in sapphire were fabricated and submitted to pulsed LiDT testing at both Quantel and SPICA – 694nm and 800nm wavelengths. Figure 12 shows SEM images of a square-grid array of mesas on a 420nm grid pitch forming an SWS ARMs texture in a 1-inch round 1mm thick sapphire window purchased from GT Crystal Systems of Salem Mass. Figure 13 shows a hexagonal grid array of mesas with a reduced grid spacing of 385nm etched in a sapphire window purchased from Guild Optical. Both samples have a feature height of about 200nm combined with a fill factor that provides peak AR performance at the laser damage test wavelengths of 694 and 800nm.

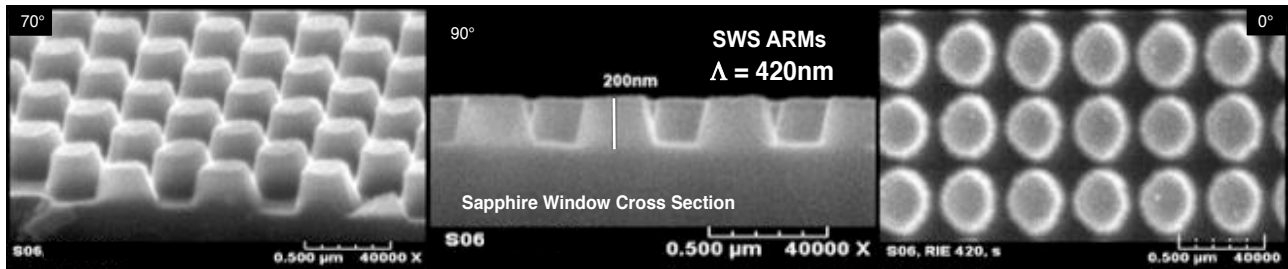


Figure 12: Elevation (70°), profile (90°), and overhead (0°) SEMs of a square-grid array of 200nm mesas etched in sapphire.

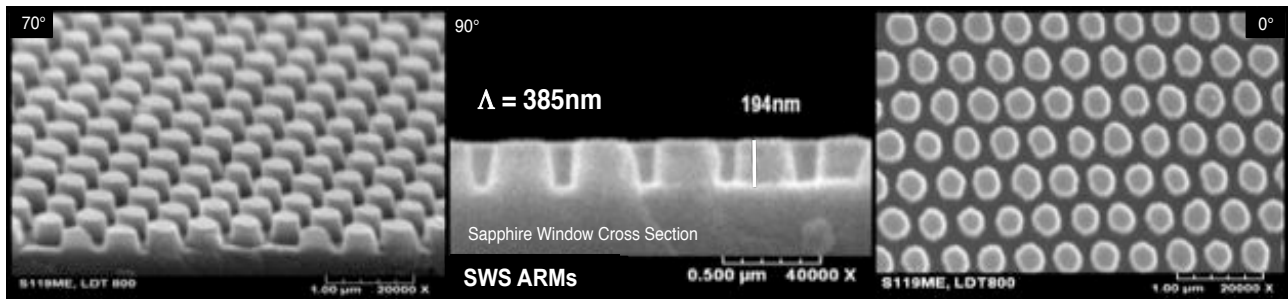
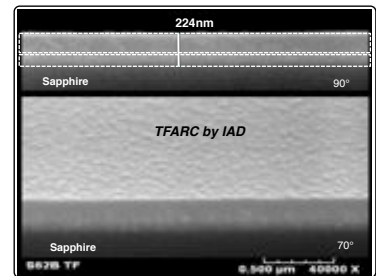


Figure 13: Elevation (70°), profile (90°), and overhead (0°) SEMs of a honeycomb array of 200nm mesas etched in sapphire.

3.2.1 694nm, 26ns Pulsed LiDT Testing: SWS ARMs Sapphire

Using the same ruby laser system described in section 3.1.2 above, Quantel conducted s-on-1 pulsed LiDT tests of four ARMs textured sapphire windows. In addition, two polished sapphire (no AR treatment) and two thin film AR coated sapphire samples were included for direct comparison. The TFARCs, purchased from Quality Thin Films (QTF) of Oldsmar Florida, were applied to multiple sapphire windows by the Ion Assisted Deposition (IAD) method. SEM images showing a cross section of the QTF two layer oxide coating on sapphire is shown here on the right. All eight samples were measured in reflection and transmission prior to 694nm LiDT testing with the results for spectral reflectivity summarized by the log plot of Figure 14. ARMs treated sapphire samples S109 (solid grey circle markers and line) and S110 (solid black line, open square markers) exhibit a reflectance of 0.1% and 0.2% respectively at the 694nm test wavelength. Samples S77 (dotted dark grey line) and S85 (solid black line, solid diamond markers), were designed for DPAL operation at longer wavelengths where reflectance levels reach as low as 0.03%. The QTF TFARC sample S63A (solid grey line) exhibits a very low reflectance minimum of 0.04% at a wavelength about 20nm longer than specified.



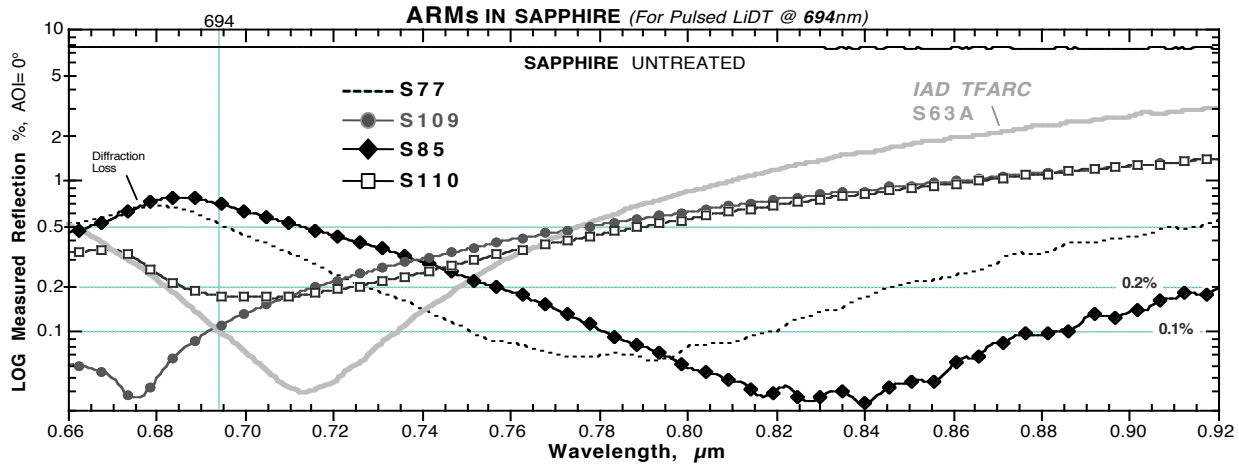


Figure 14: LOG plot of the measured reflection from sapphire windows prior to 694nm LiDT testing.

Quantel determined the pulsed LiDT at 694nm of all 8 sapphire window variants as summarized in the bar chart of Figure 15. The untreated sapphire windows (white bars labeled UT) obtained from two suppliers with a polish specified as 80-50 scratch-dig, 5 waves flatness, show good agreement with an average damage threshold of 21.5 J/cm². The four ARMs treated sapphire windows, represented by the black bars with grey dot array labeled SWS, also exhibit good agreement but at a lower average threshold of 17.5 J/cm². This result is consistent with testing of other materials at other wavelengths where a threshold 80% of the untreated surface level may be explained by non-uniformity and defects in the fabricated ARMs texture. The TFARC samples damaged with more variability and relatively high levels, with an average of 37.1 J/cm². Such a high threshold relative to the untreated surfaces was unexpected based on prior experience, but might be due to the coating covering or encapsulating sub-surface polishing damage or residual polishing marks left by the inexpensive polish – marks that can be seen in the SEM image of a laser damage site with a melted quality on the right in Figure 15.

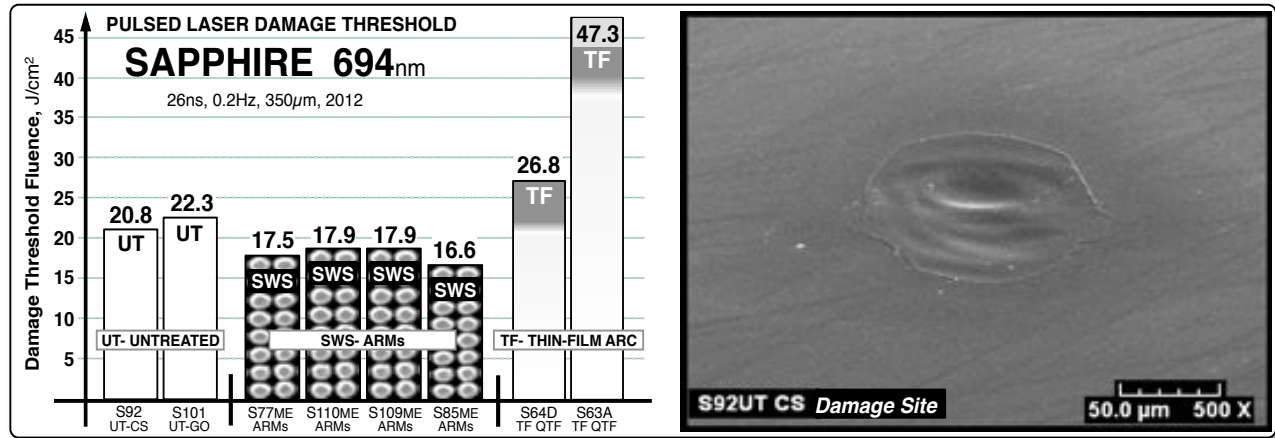


Figure 15: Left: A bar chart giving the results of the 694nm pulsed LiDT testing. Right: Damage site in untreated sapphire.

3.2.2 800nm, 10ns Pulsed LiDT Testing: SWS ARMs Sapphire

The potassium and rubidium vapors in a DPAL system have closely spaced pump and lasing wavelengths in the 765-795nm range, and a cesium vapor DPAL resonates at 894.3nm with pump light at 852.1nm. All of these wavelengths can be produced by the tunable Ti:sapphire laser operated by SPICA. To investigate the damage resistance of ARMs treated sapphire windows, the s-on-1 testing service provided by SPICA was again configured for an 800nm wavelength, 10ns pulse width, and employed to test 8 sapphire windows. The variants consisted of two untreated, 4 ARMs-treated, and two thin-film coated windows (the TFARC samples designed for peak transmission at 800nm and deposited using IAD by QTF). Figure 16 shows the measured NIR transmission of each of the test windows where the untreated sapphire window (1mm thick, solid black line) transmits between 85 and 86% over this spectral range, and the TFARC sample (solid grey line) shows a peak transmittance of 91% at 780nm. Unfortunately, TelAztec’s fiber-to-fiber based spectrometer covering the visible-NIR spectrum exhibits a high level of noise particularly at the long wavelength

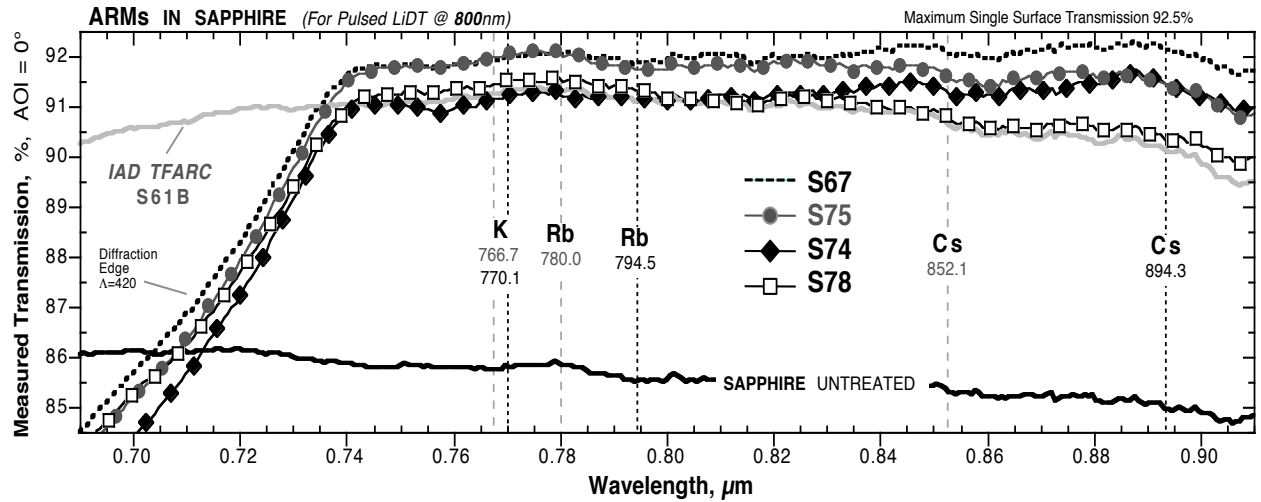


Figure 16: Plot of the measured spectral transmission of sapphire windows with ARMs in 1 surface prior to 800nm LiDT testing.

end of its range where the grating within the spectrometer has very low efficiency. In reflection measurements the noise level can be reduced dramatically with a built in referencing method that allows the full dynamic range of the spectrometer to be used over the low light signal range typical of surface reflections. Transmission measurements must divide the dynamic range over a 100% signal reference that is typically 20 times larger than reflection measurements – leading in part to the $\pm 1\%$ noise level. So from the more accurate reflection measurements we know that the performance of the ARMs treated and TFARC surfaces is quite good, similar to that shown in Figure 14 with all samples exhibiting no more than 0.1 to 0.2% loss. Even with significant upgrades to the spectrometer hardware, transmission measurements accurate to 1 part in 1000 are very difficult to attain. However, the transmission measurements of Figure 16 are instructive in that they show the loss due to free-space diffraction from the periodic array, and they would indicate losses due to scattering from surface defects as a decreasing transmission at shorter wavelengths. And of course any absorption at the surface or in the bulk would also be indicated in transmission.

Figure 17 shows a bar chart summarizing the damage threshold data collected by SPICA over a many week test period. As with previous bar charts, the untreated window surfaces are indicated by the white bars with the UT label, the ARMs-treated samples are shown as black bars with a white dot array labeled SWS, and the TFARC samples are shown as solid white bars with a grey top labeled TF. SPICA had a great deal of difficulty setting the spot size that would damage the samples in a consistent manner to allow several data points above and below the damage onset threshold. Because of these early issues and multiple system re-calibrations, SPICA re-tested all 8 samples after establishing the test parameters yielding the most consistent results. The re-test data is plotted as grey bars along side the final data listed on each certificate. Note that the spot size used (indicated at the bottom of each bar) still varied from 206 μm down to 62 μm where statistically, scanning the smaller spot size should avoid more surface defects and yield slightly higher damage thresholds.

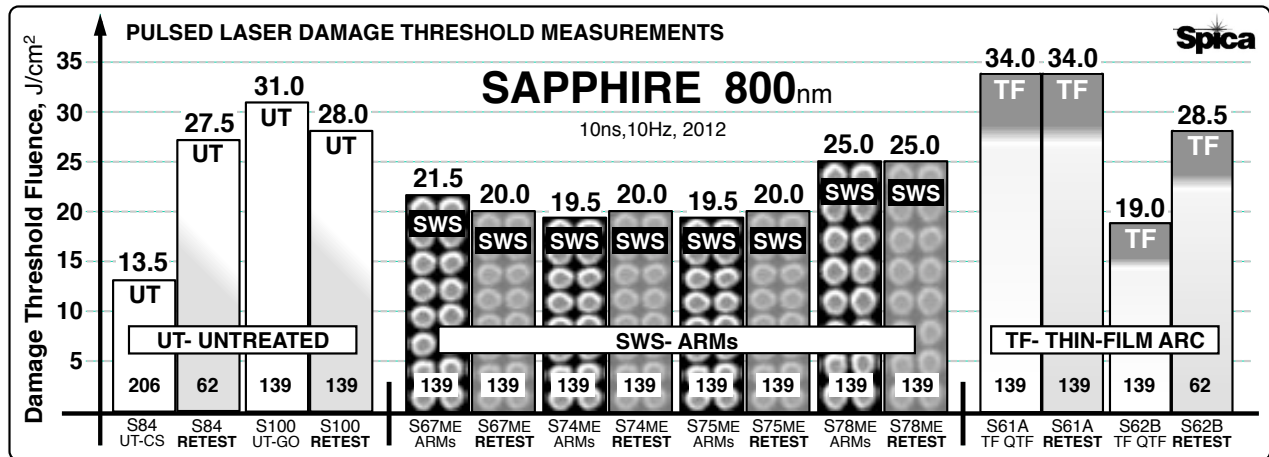
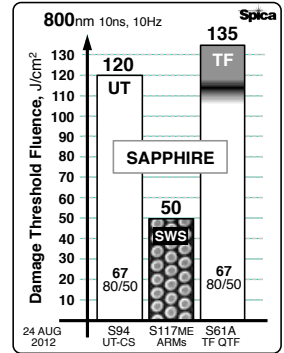


Figure 17: Bar chart showing the measured LiDT of untreated, ARMs-treated and TFARC sapphire windows at 800nm.

Neglecting the very first untreated sample data collected by SPICA using the largest spot size, we find the average damage threshold of the ARMs-treated sapphire windows of 21.3 J/cm², to be about 75% of the average untreated surface threshold of 28.8 J/cm², values consistent with the 694nm tests and prior work at 1064nm. As before this is expected to be an issue with ARMs texture uniformity and defect level, which should improve with further process development. Even with one inconsistent test result, the TFARC samples fared surprisingly well exhibiting an average threshold of 31.3 J/cm². This SPICA testing result is consistent with the Quantel 694nm results for the TFARC samples, but is not consistent with the literature for other substrate materials that generally shows thin film AR coatings failing at a fraction of the fluence required to damage a polished substrate.

In an effort to quickly to confirm this result, three more sapphire windows, one untreated, one ARMs treated, and one TFARC window, were submitted to SPICA for a repeat test at the smallest spot size. The test results were anomalous in that the measured threshold levels were four times higher for the untreated and TFARC samples, but only two times higher for the ARMs treated samples as shown by the bar chart on the right. Although the high threshold values indicate some unknown system calibration error, the TFARC level was again about 10% higher than the untreated sapphire, a result that is consistent with the previous more extensive testing.



Based on the unexpected TFARC results in the 694nm and 800nm pulsed LiDT testing, a concept was evaluated of first depositing a refractive index matching thin film on the sapphire substrate surface that would serve to bury or encapsulate residual polishing defects or subsurface damage, and then to fabricate ARMs in this protective layer. A thin film of aluminum oxide, Al₂O₃, was selected as the coating material because it is a close match to the refractive index of sapphire (crystalline Al₂O₃), and is expected to have thermal, mechanical, and chemical durability properties similar to sapphire for use in the DPAL HEL application. RCWA optical propagation modeling was used to examine the combination of ARMs fabricated in commercially deposited Al₂O₃ films on sapphire. Figure 19 gives the predicted normal incidence reflection of the four ARMs in Al₂O₃ on sapphire shown in cross section in Figure 18. From left to right the design variants are; 1) a Motheys-type pyramid array on a 385nm pitch etched fully through a 560nm thick Al₂O₃ film with a predicted spectral reflectivity shown as the grey line with open triangle markers; 2) Motheys pyramids again defined on a 385nm pitch but etched only 350nm deep into a 650nm thick Al₂O₃ layer, with predicted reflectivity indicated by the black line and solid black triangle markers; 3) an SWS-type hole array defined on a 385nm grid etched just 150nm deep in a 650nm thick Al₂O₃ layer, with predicted reflectivity indicated by the dashed grey line; and 4) an SWS-type post array on a 385nm grid etched 150nm deep into a 450nm thick Al₂O₃ film with predicted reflectivity given by the dotted black line.

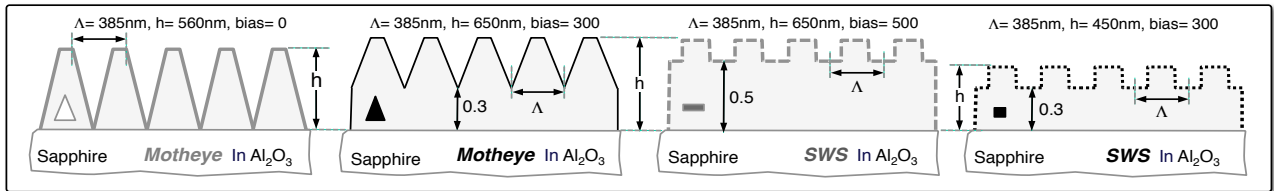


Figure 18: Cross sections of four ARMs design variants etched into an Al₂O₃ layer deposited on sapphire.

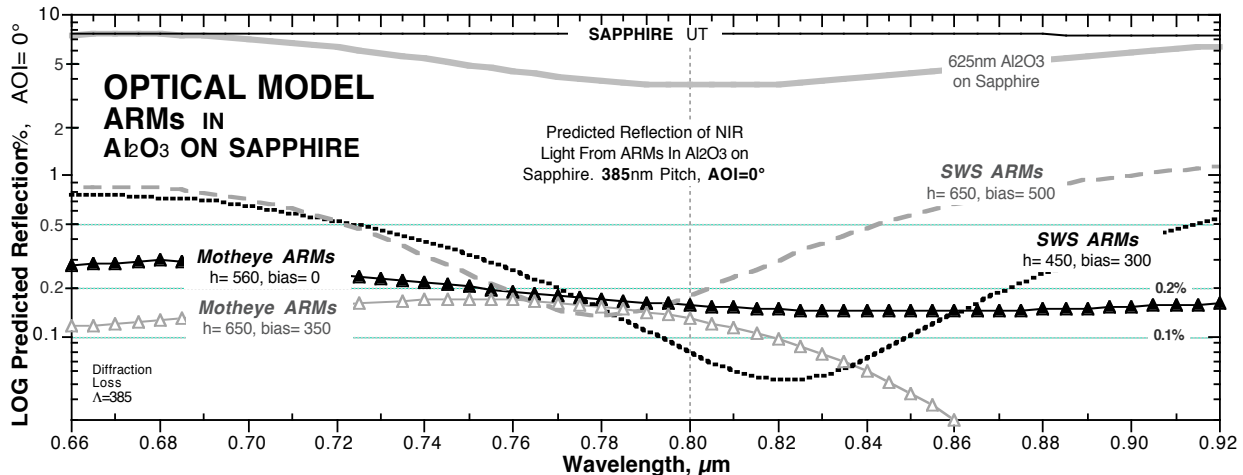


Figure 19: Predicted reflection of ARMs variants etched into an Al₂O₃ layer deposited on sapphire – designed for 800nm.

Reflection levels below 0.2% at the target 800nm test wavelength are predicted for all four cases where the performance bandwidth of the Motheye textures is as expected, much larger than the SWS ARMs designs. Because the deeper Motheye textures are more difficult to fabricate with current processes, and because thicker Al₂O₃ layers may afford greater protection against laser damage, the third design based on a 625nm thick film and SWS-type ARMs was chosen for the concept verification tests. Figure 19 also shows the predicted normal incidence spectral reflection of a uniform 625nm thick Al₂O₃ layer on sapphire (solid grey line) where the Al₂O₃ film refractive index was provided by QTF as being typical of their coatings done by IAD.

Sapphire substrates obtained from Guild Optical were first coated by QTF with a 625nm thick Al₂O₃ layer, and then processed with SWS ARMs optimized for maximum transmission at 800nm. Figure 20 shows two rows of SEM images of the same ARMs textured Al₂O₃ layer on sapphire window before (top) and after (bottom) cleaning procedures to remove residual metal mask material used in the ARMs etching process. (Note that SEM image distortion causes the illusion of a curved Al₂O₃ layer.) Despite the many pattern defects that can be seen in the SEM images, the sample reflectivity was reduced to a level below 0.1% at 790nm as given by the dashed black line in Figure 21. The measured reflection of both the ARMs-treated and the untreated (solid grey line) Al₂O₃ films on sapphire were also a good match to the predicted performance indicated by the dotted black lines. These samples were submitted to SPICA for a second round of damage testing at 800nm along with multiple untreated sapphire windows with different polish levels, and an ARMs treated sapphire window with increased pattern uniformity and reduced defects resulting from fabrication process improvements. The measured reflectivity of these samples is also shown in Figure 21 with the ARMs in sapphire (black triangle markers) and TFARC samples (solid grey line) exhibiting losses below 0.05% at 800nm.

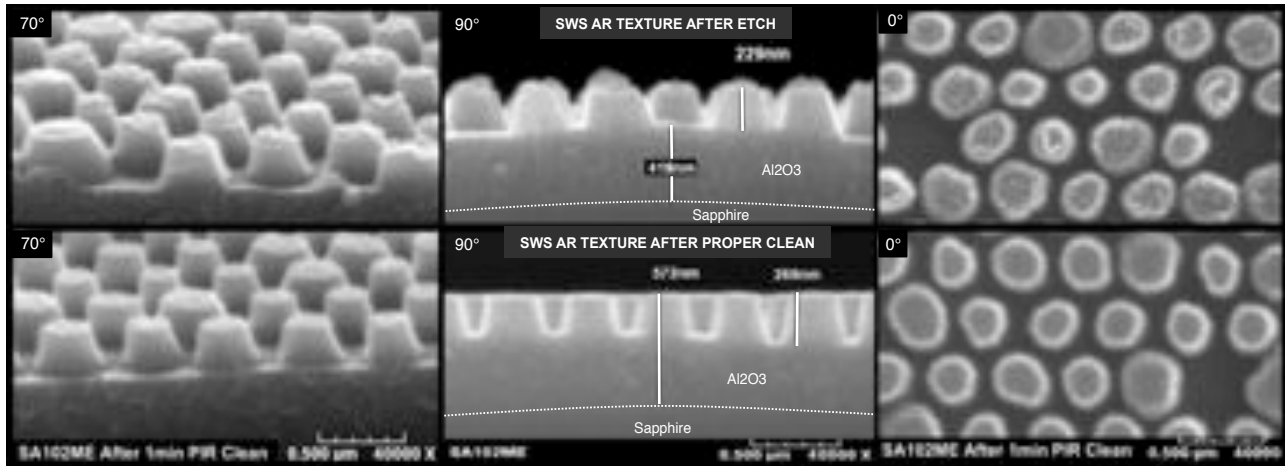


Figure 20: SEMs of ARMs in an Al₂O₃ layer on sapphire before (top) and after (bot) cleaning to remove residual process metal.

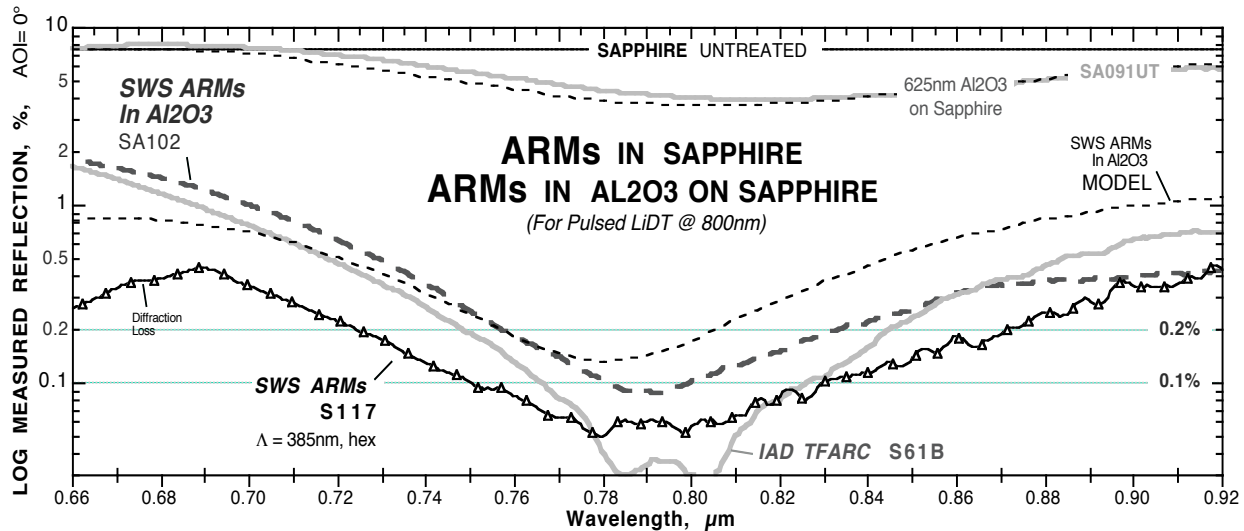
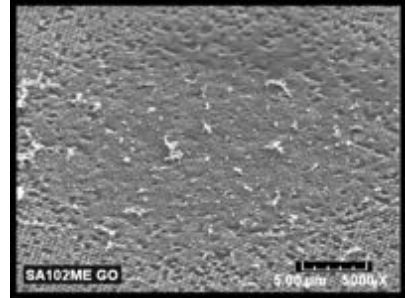


Figure 21: LOG plot of the measured reflection from improved ARMs etched in sapphire windows prior to 800nm LiDT testing.

S-on-1 damage tests of the Al₂O₃ on sapphire samples showed dramatic results as can be seen in the bar chart of Figure 22. The three far right bars represent an untreated Al₂O₃ film on sapphire (SA91UT), a partially cleaned ARMs-treated Al₂O₃ film on sapphire (SA102), and a *retest* of sample ARMs-treated SA102 after additional further acid cleaning. The initial 4.0 J/cm² result (2nd from right) for SA102 was remarkably low. Inspection of the sample after LiDT testing revealed very small and uncharacteristic damage sites. Suspecting that the sample had surface contamination, a section of SA102 was broken off for SEM analysis. One of the damage sites is shown in the low magnification SEM on the right where an unusual type of debris was found on top of a depression that has a melted or fused appearance. The higher magnification SEM images in the top row of Figure 20 confirm that the metal mask material used in the ARMs etch process had not been fully stripped and mostly likely induced the low LiDT due to surface absorption. The remaining section of sample SA102 was re-cleaned in acid and resubmitted for LiDT testing yielding a 10x increase in the threshold recorded at 41 J/cm², or 72% of both the untreated Al₂O₃ film on sapphire window (grey tipped white bar, #SA91UT) and the as received untreated sapphire substrate (white bar, #S104UT). This result is very encouraging, as the sample was a one-off prototype with processing defects, yet the LiDT compared favorably with the TFARC substrate (grey and black tipped white bar labeled TF, #S62CTF), confirming – at least with one data point – the protective effect of the thin-film. Further ARMs fabrication process improvements could then be expected to yield even higher thresholds comparable to the untreated film layer.



In an attempt to understand if the high thresholds found with thin-films on sapphire were simply related to the poor initial surface polish, additional untreated samples were included in the test. Two sapphire substrates (S148UT, and S149UT) with a high level of polish specified as 10/5 scratch-dig, 1/4 wave flatness, were provided by GT Crystal Systems and submitted to SPICA in as-received condition with no further cleaning. Another two sapphire substrates (S120UT, and S121UT) were salvaged from prior work through grinding and polishing by Guild Optical to a level of 20/10 scratch-dig, 1 wave flatness. Sample S120UT was submitted to SPICA after only solvent rinsing and nitrogen blow drying, whereas the second sample, S121UT, was aggressively cleaned in sulfuric acid and peroxide prior to the SPICA testing. As mentioned above, a fifth untreated sample with just a simple 80/50 scratch-dig, 5 wave flatness specification, S104UT was submitted for further comparison. Surprisingly, this lowest level of polish exhibited the highest damage threshold of 55 J/cm², a result which is not consistent with the prior testing of the same substrates with identical polish specifications. Even neglecting this result as anomalous, there was no clear correlation of damage threshold and polish level in this limited sample set. Only the additional cleaning of the 20/10 sample S121UT indicates the well-known impact of surface preparation and cleanliness on damage threshold. The next steps will be to fabricate ARMs in a statistically relevant number of highly polished sapphire substrates and compare these with TFARCs deposited on the sample highly polished surfaces.

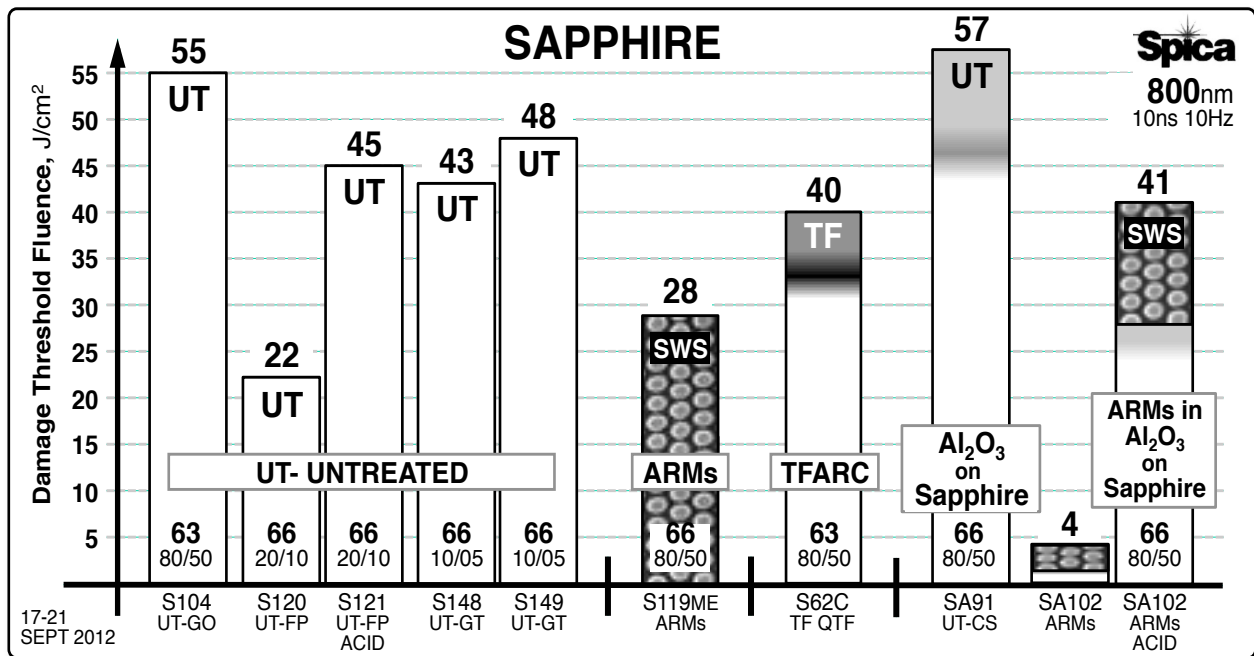


Figure 22: Bar chart showing further results of LiDT testing of untreated and ARMs-treated sapphire windows at 800nm.

3.3. ARMs in Nd:YAG and SPINEL.

Aperture and power scaling for solid state HEL systems based on metal ion doped yttrium aluminum garnet (YAG) gain material, requires the difficult and expensive growth of larger area single crystals, or the production of less expensive but often less durable poly-crystalline ceramics. YAG laser output power is also currently limited by the low damage resistance of TFARCs. ARMs textures built in YAG gain media offer a single material solution without the differential absorption, loss of adhesion, and water vapor absorption issues that limit TFARC reliability. In collaboration with the Naval Research Laboratory (NRL), the pulsed laser damage resistance of ARMs in both single crystal and ceramic Neodymium (Nd) doped YAG was investigated at wavelengths of 1064nm and 1538nm using the standardized testing services of Quantel.

A second ceramic material important to HEL systems due to its wide visible thru mid-IR transmission bandwidth and exceptional mechanical durability rivaling sapphire, is magnesium aluminate spinel ($MgAl_2O_4$) commonly known as SPINEL. NRL has been developing HEL applications for SPINEL that typically involve its use as an external window isolating HEL components from harsh environments^[30,31]. NRL's SPINEL can be produced with low surface and bulk absorption at the HEL wavelengths 1030nm and 1064nm produced by ytterbium Yb:YAG and Nd:YAG lasers. ARMs textures in SPINEL offer the low back reflections critical for HEL systems combined with the inherent laser damage resistance and environmental durability of the bulk SPINEL material.

NRL provided polished discs of single and polycrystalline Nd:YAG material as well as polished windows of their proprietary SPINEL. Additional SPINEL material was purchased as unfinished blanks from Technology Assessment And Transfer Company (TA&T) and subsequently polished to a 40/20 scratch-dig, 2 wave flatness specification by Opticraft Incorporated of Woburn Massachusetts. SWS-type ARMs consisting of honeycomb arrays of mesas were designed and fabricated in these materials as illustrated by the SEM images of Figure 23.

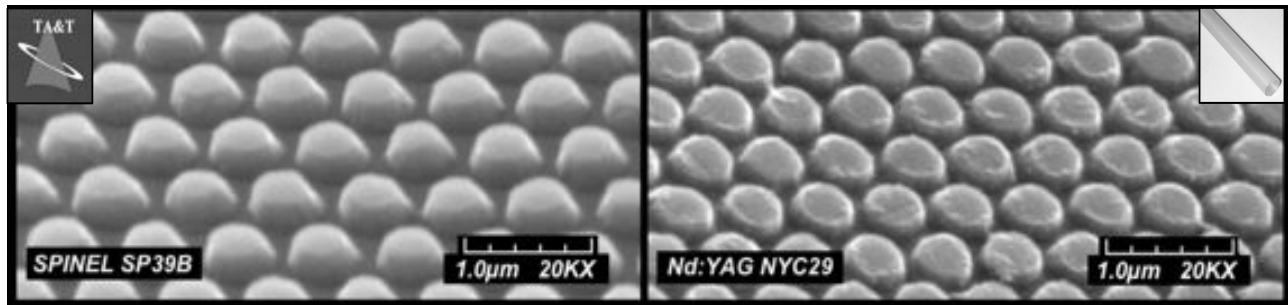


Figure 23: SEMs of ARMs in SPINEL (left) and Nd:YAG (right) prior to LiDT tests at 1064nm.

Because of the limited number of Nd:YAG samples available for process development, the ARMs performance was not fully optimized prior to the 1064nm damage testing as illustrated by the measured spectral reflection data shown in Figure 24. The process for fabricating SWS ARMs textures in SPINEL did yield high performance samples, with reflection losses in the range of 0.06% to 0.3% at 1064nm as indicated by the dotted grey curve, the black curve with solid square markers and the black curve with open square markers shown in the figure.

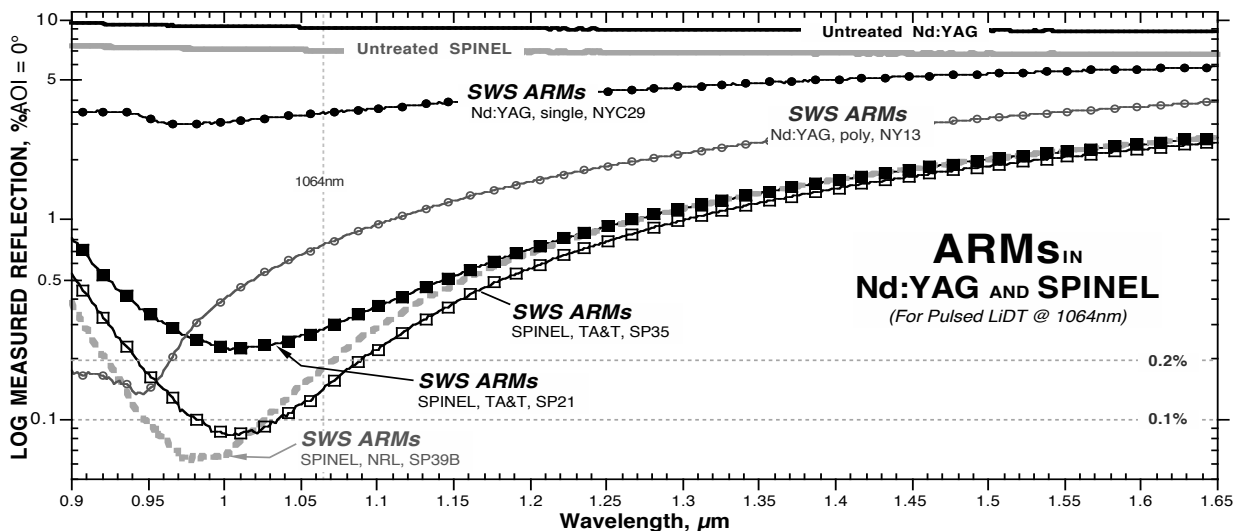


Figure 24: Measured reflection (log scale) of untreated and ARMs treated YAG and Spinel – 1064nm LiDT tests

3.3.1 **1064nm, 10ns and 1538nm, 14ns Pulsed LiDT Testing: ARMs in Nd:YAG and SPINEL**

The Nd:YAG discs supplied by NRL were between 9 and 10mm diameter, presumably sliced from a laser rod to a thickness between 1 and 2mm, and then polished to an unknown polish specification – but likely no better than 80/50 scratch-dig, 5 waves flatness. The parts were however generally free of surface pits as inspected with an optical microscope at the 150X magnification used to observe surface damage during the s-on-1 testing. Only four discs were submitted to Quantel for testing at 1064nm; one untreated and one ARMs treated disc of both single crystal and polycrystalline material. Results of the Quantel testing are shown in the bar chart on the left of Figure 25, where the test parameters were; 1064nm wavelength, 10ns pulse duration, 20Hz repetition rate, 0.5mm spot size, TEM₀₀, multiple longitudinal modes, linear polarization, AOI=0°, 50-60 sites, 200 shots/site. A reduced number of sites were exposed due to the larger spot size and smaller area samples. Very low damage thresholds between 3.1 and 4.6 J/cm² were found for all four discs with no indication that single crystal material was more durable than polycrystalline material as was expected from the single crystal sapphire data previously reported^[19] and reproduced for comparison in the bar charts on the right of both Figures 25 and 26. It is likely that residual polishing damage and surface preparation is again the dominant factor in determining pulsed laser damage resistance. Note also the high damage threshold of 20.8 J/cm² recorded for a QTF deposited single layer TFARC on Yb:YAG relative to the as polished, untreated material. This threshold level is the same as that specified by VLOC for their TFARC on Nd:YAG products^[32]. These results suggest that if processes for polishing and sub-surface damage removal proven effective for doubling the laser damage resistance of fused silica material, cannot be practically achieved in ceramics, then the strategy described at the end of the sapphire section 3.2.2 above of fabricating ARMs within a YAG or Al₂O₃ thin film layer deposited over the Nd:YAG surfaces may be a practical path toward realizing higher laser damage resistance with little compromise to the inherent bulk material mechanical and chemical durability.

Four polycrystalline SPINEL windows, two supplied by NRL and two purchased from TA&T, each 1-inch round by 1-2mm thick, were also submitted for damage testing by Quantel. Each window was marked to allow testing at 1064nm on one half, and testing at 1538nm on the opposite half. All four windows exhibited low damage thresholds similar to the Nd:YAG results at both wavelengths as shown in the bar graph of Figure 26. The TA&T SPINEL windows fared slightly better than the NRL windows at both wavelengths likely due to the higher polish level of the TA&T material.

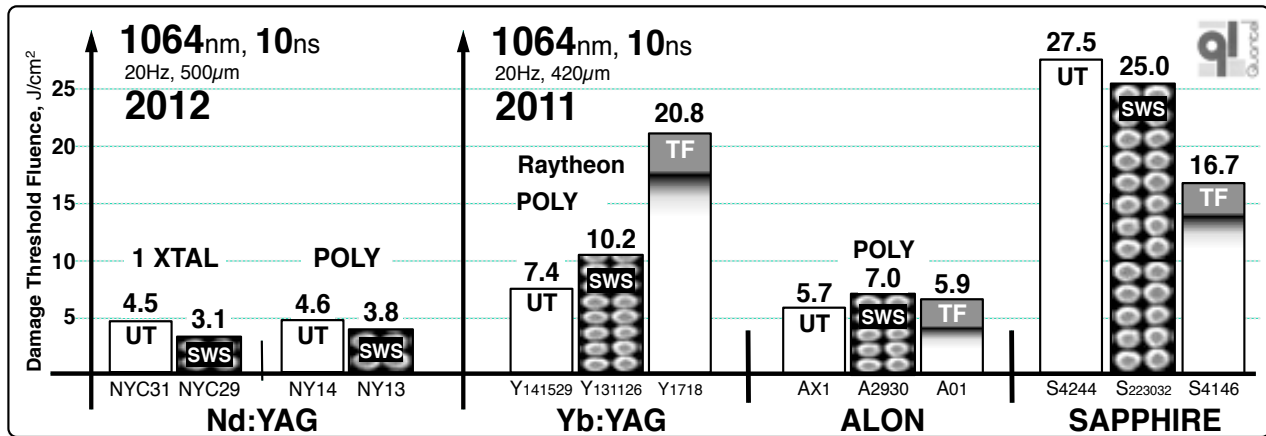


Figure 25: Bar chart showing the LiDT of untreated and ARMs treated Nd:YAG windows at 1064nm, 10ns.

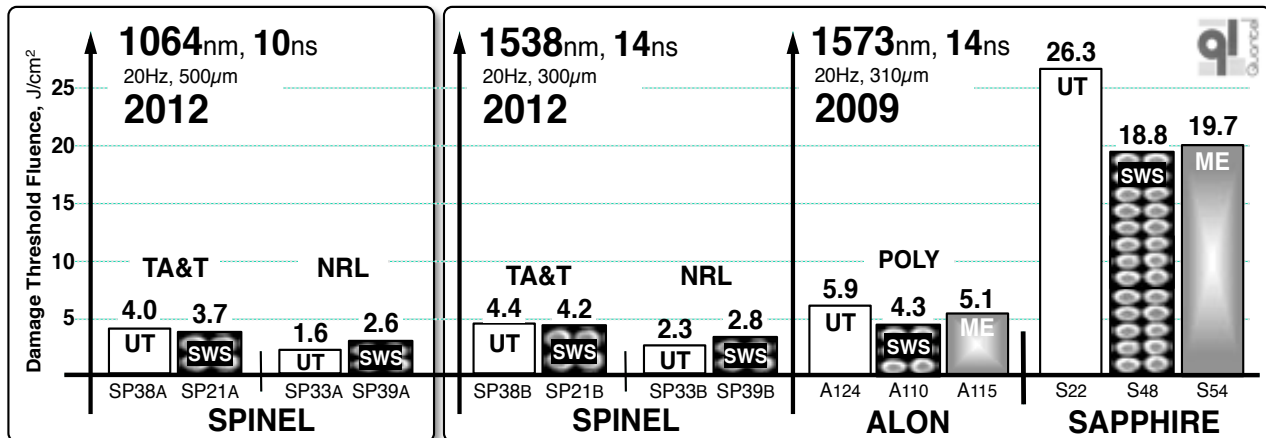


Figure 26: Bar chart showing the LiDT of untreated and ARMs treated Nd:YAG windows at 1538nm, 14ns.

An additional issue affecting the laser damage resistance of ceramics is the weakness of the boundaries between the various crystal orientations known as grains. Figure 27 shows SEM views of damage sites produced during the s-on-1 testing for the polycrystalline SPINEL (left) and Nd:YAG (right), and the single crystal Nd:YAG (center). The upper row of SEMs are overhead views taken at a 500X magnification, and the lower row of SEMs are higher magnification elevation views showing the detail of a part of each damage site where the ARMs features can be distinguished. Damage from the laser exposure in SPINEL propagates well beyond the surface causing ejection of what appears to be entire crystal grains whose boundaries form the sharp edges. Some melting and reflow of the surface is evident along the edges. In contrast the Nd:YAG laser damage sites appear to be only melted or fused in both the single and polycrystal materials with little evidence of the collateral grain boundary damage seen with the SPINEL. This may be due to a smaller grain size in the poly-crystal Nd:YAG. The higher laser damage resistance of the TFARC on Yb:YAG might be attributable to a strengthening of the grain boundaries through encapsulation by the coating – a method that is common for increasing resistance to erosion by sand impacts in poly-crystal materials such as ZnSe and ZnS^[33].

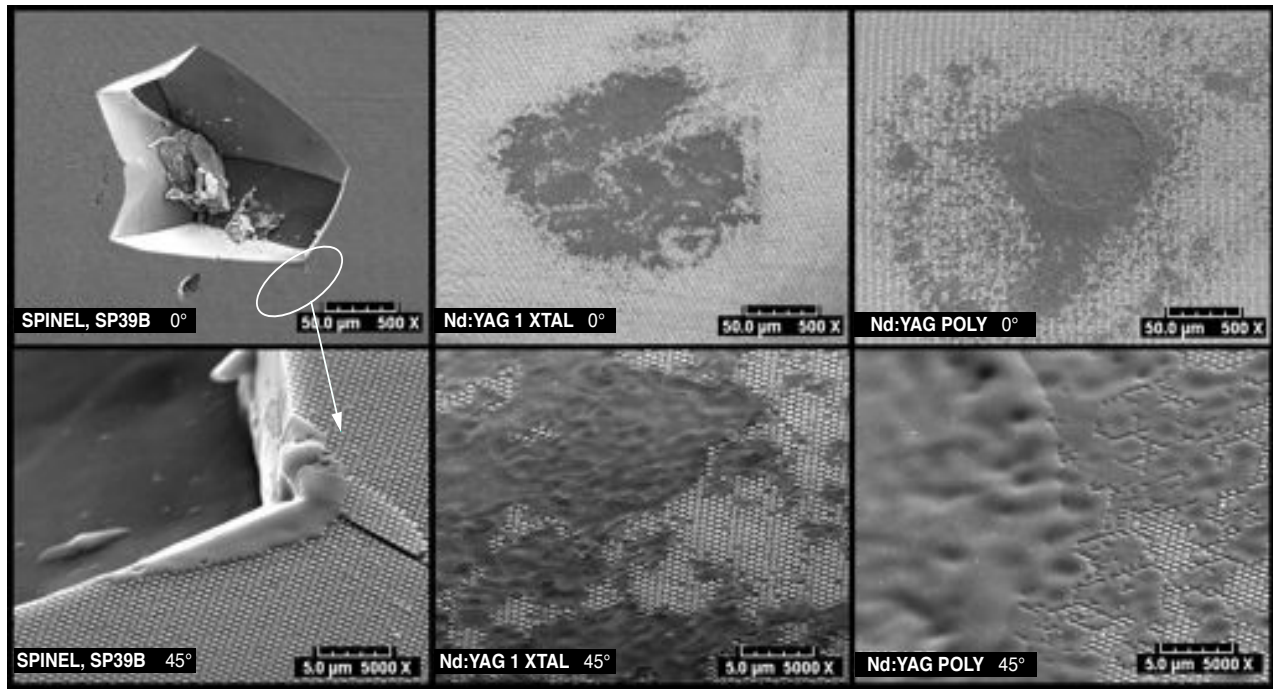


Figure 27: Overhead (top row) and elevation (bot. row) views of laser damage sites in SPINEL (left) & Nd:YAG (center, right).

4.0 SUMMARY

Laser power scaling, bandwidth requirements, and reliability concerns continue to drive the adoption of optical microstructure technology. AR Microstructures (ARMs) in particular show promise as a durable, high performance, polarization insensitive, omni-directional, wide-bandwidth alternative to thin-film AR coatings (TFARC). Random ARMs in fused silica were shown to have a pulsed laser damage resistance between 3 and 5 times higher than TFARCs in third party testing conducted at wavelengths of 532nm, 694nm, 800nm, 1064nm, and 1538nm by the Army Research Laboratory, Quantel USA, and SPICA Technologies. ARMs in both fused silica and Schott N-BK7 materials are nearly qualified for laser optics offered by commercial catalog companies. Lastly, efforts to combine the laser damage resistance and performance of ARMs with the inherent chemical and mechanical durability of sapphire optics, ceramic SPINEL windows, and YAG laser gain media, have shown that polishing and post polishing surface preparation processes remain the dominant factors in determining the survivability of these materials in HEL systems.

5.0 ACKNOWLEDGEMENTS

The authors gratefully acknowledge the support provided by the ARMY Research Laboratory, Survivability/Lethality Analysis Directorate, White Sands Missile Range, NM, through the efforts of Norman Comer and Christopher Zella who conducted the 532nm pulsed damage testing reported. Major support for this ARMs work is being provided by the High Energy Laser Joint Technology Office under a 2011 Advanced Concepts BAA, contract FA9451-12-D-0196 (Cleared for Public Release # 377ABW-2012-1409 dated 02NOV2012). Jeff Runkel of Quantel USA (JRunkel@quantelusa.com) is also gratefully acknowledged for his fast and thorough work providing the certified,

NIST traceable LiDT testing service at four different wavelengths. The authors also thank Michael Thomas and Andrew Griffin of SPICA Technologies for their major efforts to obtain the detailed and consistent 800nm LiDT testing data presented. Dr. Jasbinder Sanghera and Catalin Florea of the Naval Research Laboratory are acknowledged for their support of the ARMs in Nd:YAG and SPINEL projects. The SEM images shown were carefully recorded by Mr. John Knowles of MicroVision Laboratories Inc. of Chelmsford Mass.

6.0 REFERENCES

- [1] Stolz, C. J., Caputo, M., Griffin, A.J., and Thomas, M.D. "BDS Thin Film UV Antireflection Laser Damage Competition," Proc. SPIE **7842**, 784206 (2010)
- [2] Ciapponi, A., et.al., "S on I testing of AR and HR designs at 1064 nm," Proc. SPIE **7842**, 78420J (2010)
- [3] Stolz, C. J., Adams, J., Shirk, M. D., Norton, M. A., Weiland, T. L. "Engineering meter-scale laser resistant coatings for the near IR (LLNL)," Proc. SPIE **5963**, (2005)
- [4] Zweiback, J., Komashko, A., and Krupke, W.F., "Alkali vapor lasers," Proc. SPIE **7581**, 75810G (2010)
- [5] Zhdanov, B.V., and Knize, R.J., "Alkali Lasers Development at the Laser and Optic Research Center of the US Air Force Academy," Proc. SPIE **7005**, 700524 (2008)
- [6] Shinn, M., et. al., "Xtreme optics: the behavior of cavity optics for the Jefferson Lab Free-Electron Laser," Proc. SPIE **6403**, 64030Y (2006)
- [7] Turner, T. and Damery, M., "Thin-Film Coatings: A Buyer's Guide," Photonics Handbook <http://photonics.com/edu/Handbook.aspx?AID=42399>
- [8] Moskalev, I.S., Fedorov, V.V., and Mirov, S.B., "Tunable, Single-Frequency, and Multi-Watt Continuous-Wave Cr²⁺:ZnSe Lasers," Optics Express **16**, 4145-4153 (2008)
- [9] Wagner, T. J., et. al., "Measurement and modeling of infrared nonlinear absorption coefficients and laser-induced damage thresholds in Ge and GaSb," JOSA B, **27**, 2122-2131 (2010)
- [10] Hobbs, D.S., and MacLeod, B.D., "Design, Fabrication and Measured Performance of Anti-Reflecting Surface Textures in Infrared Transmitting Materials," Proc. SPIE **5786**, (2005)
- [11] Hobbs, D.S., and MacLeod, B.D., "Update on the Development of High Performance Anti-Reflecting Surface Relief Micro-Structures," Proc. SPIE, Vol. **6545**, (2007)
- [12] Hobbs, D.S., "Laser Damage Threshold Measurements of Microstructure-Based High Reflectors," Boulder Damage Symposium XL, Proc. SPIE **7132**, (2008)
- [13] Hobbs, D.S., and MacLeod, B.D., "Long Life, High Performance Anti-Reflection Treatment for HgCdTe Infrared Focal Plane Arrays," Proc. SPIE **6940**, (2008)
- [14] Lowdermilk, W.H. and Milam, D., "Graded-index antireflection surfaces for high-power laser applications," Appl. Physics Letters, **36** (11), 891 (1980).
- [15] Cook, L.M., et.al., "Integral Antireflective Surface Production on Optical Glass," Journal of the American Ceramic Society, **65** (9), c152 (1982).
- [16] Hobbs, D.S., and MacLeod, B.D., "High Laser Damage Threshold Surface Relief Micro-Structures for Anti-Reflection Applications," Proc. SPIE **6720**, 67200L (2007).
- [17] Hobbs, D.S., "Laser damage threshold measurements of anti-reflection microstructures operating in the near UV and mid-infrared," Proc. SPIE **7842**, 78421Z (2010)
- [18] Hobbs, D.S., "Study of the Environmental and Optical Durability of AR Microstructures in Sapphire, ALON, and Diamond," Proc. SPIE **7302**, 73020J (2009)
- [19] Hobbs, D.S., et.al., "Laser damage resistant anti-reflection microstructures in Raytheon ceramic YAG, sapphire, ALON, and quartz," Proc. SPIE **8016**, 80160T (2011)
- [20] MacLeod, B.D., Hobbs, D.S., and Sabatino, E. "Moldable AR microstructures for improved laser transmission and damage resistance in CIRCM fiber optic beam delivery systems," Proc. SPIE **8016**, 80160Q (2011)
- [21] Du, Y., et.al., "Laser-induced damage properties of antireflective porous glasses," Proc. SPIE **8206**, 82060Q (2012)
- [22] Wilson, S.J., Hutley, M.C., "The optical properties of 'moth eye' antireflection surfaces," Optica Acta, **29**, 7 (1982)
- [23] Hobbs, D.S., et. al., "Automated Interference Lithography Systems for Generation of Sub-Micron Feature Size Patterns," Proc. SPIE **3879**, 124 (1999)
- [24] ThorLabs, "webpage," http://www.thorlabs.com/newgrouppage9.cfm?objectgroup_id=1121
- [25] EdmundOptics, "webpage," <http://www.edmundoptics.com/optics/windows-diffusers/laser-line-windows/1-20-high-power-laser-line-windows/2753?PageNum=2&Sort=displayOrder&Order=asc#products>
- [26] Newport, "webpage," http://search.newport.com/?q=*&x2=sku&q2=10QW20-1
- [27] CVI-Melles-Griot, "webpage," SPECS tab: <https://www.cvimellesgriot.com/Products/Laser-Windows.aspx>
- [28] RMI, "webpage," <http://rmico.com/coatings-specifications/vis-nir-coatings/visnir-narrowband-anti-reflection>
- [29] PrecisionPhotonics, "downloadable catalog," <http://www.precisionphotonics.com/Catalog.pdf>, pgs 12-13
- [30] Aggarwal, I., et.al., "SPINEL AS EXIT APERTURE WINDOW FOR HEL SYSTEMS," NRL Report, <http://www.dtic.mil/cgi-bin/GetTRDoc?AD=ADA494870>, (2008)
- [31] Sanghera, J. et al., "Transparent ceramics for high-energy laser systems," Optical Materials **33**, 511-518 (2011)
- [32] VLOC-Company, "brochure," available online at: <http://www.vloc.com/PDFs/YAGBrochure.pdf>, page 5
- [33] Hobbs, D.S., MacLeod, B.D., and Ondercin, R.J., "Initial Erosion Studies of Microstructure-Based Anti-Reflection Treatments in ZnS," 12th DoD Electromagnetic Windows Symposium, (2008)